V393
.R46

MIT LIBRARIES
3 9080 02753 0291

Report 1849

DEPARTMENT OF THE NAVY

DAVID TAYLOR MODEL BASIN
WASHINGTON, D.C.

HYDROMECHANICS

AERODYNAMICS

STRUCTURAL MECHANICS

APPLIED MATHEMATICS

ACOUSTICS AND VIBRATION

WAKE ANALYSIS OF SHIP MODELS
SINGLE-SCREW DE-TYPE

MASS. INST. OF TECHNOLOGY
JUN 23 1976
PARKER ENGINEERING LIBRARY

By

H. M. Cheng and J. B. Hadler

HYDROMECHANICS LABORATORY

RESEARCH AND DEVELOPMENT REPORT

June 1964

Report 1849

PRNC-TMB-648 (Rev 1-64)

WAKE ANALYSIS OF SHIP MODELS
SINGLE-SCREW DE-TYPE

by

H. M. Cheng and J. B. Hadler

June 1964

Report 1849

TABLE OF CONTENTS

	Page
ABSTRACT	1
INTRODUCTION	1
TEST PROCEDURES	3
REDUCTION OF DATA	4
PRESENTATION OF DATA	9
APPLICATION OF WAKE DATA IN PROPELLER-SHIP DESIGNS	9
RESULTS OF ANALYSES	13
CONCLUSIONS AND RECOMMENDATIONS	16
ACKNOWLEDGMENTS	17
REFERENCES	18

LIST OF FIGURES

Figure 1 - Arrangement of Pitot Tube Assembly	20
Figure 2 - Coordinate System of Velocity Components	21
Figure 3 - Velocity Diagram	6
Figure 4 - Lines of Single-Screw DE-Type Ships	22
Figure 5 - Wake Velocity Diagram and Test Data, Model 4360	23
Figure 6 - Wake Velocity Diagram and Test Data, Model 4554	24
Figure 7 - Wake Velocity Diagram and Test Data, Model 4773	25
Figure 8 - Wake Velocity Diagram and Test Data, Model 4870	26
Figure 9 - Wake Velocity Diagram and Test Data, Model 4881	27
Figure 10- Wake Velocity Diagram and Test Data, Model 4954	28

Figure 11 - Circumferential Longitudinal (V_x/V) and Tangential (V_t/V) Velocity Distributions at Various Test Radii, Model 4360 29

Figure 12 - Circumferential Longitudinal (V_x/V) and Tangential (V_t/V) Velocity Distributions at Various Test Radii, Model 4554 30

Figure 13 - Circumferential Longitudinal (V_x/V) and Tangential (V_t/V) Velocity Distributions at Various Test Radii, Model 4773 31

Figure 14 - Circumferential Longitudinal (V_x/V) and Tangential (V_t/V) Velocity Distributions at Various Test Radii, Model 4870 32

Figure 15 - Circumferential Longitudinal (V_x/V) and Tangential (V_t/V) Velocity Distributions at Various Test Radii, Model 4881 33

Figure 16 - Circumferential Longitudinal (V_x/V) and Tangential (V_t/V) Velocity Distributions at Various Test Radii, Model 4954 34

Figure 17 - Mean Longitudinal Velocity ($\overline{V}_x/V$), Calculated Volumetric Velocity ($\overline{V}_v/V$) and Volumetric Mean Wake Velocity ($1-W_x$) 35

Figure 18 - Amplitudes of Various Harmonics of Longitudinal (V_x/V) and Tangential (V_t/V) Velocity Components 36

Figure 19 - Mean Advance Angle ($\overline{\beta}$), Variations in Beta Angle ($\Delta\beta$) and Pressure Factor (P) 37

Figure 20 - Variation in Beta Angle ($\Delta\beta$) and Pressure Factor (P) for Various J_a Values 38

NOTATION

D	Propeller diameter
J_a	Apparent advance coefficient V/nD
n	Propeller revolutions
P	Pressure factor $(V_b^2)_{max} / \overline{V_b^2} - 1$
R	Radius of propeller
r	Radial coordinate
U	Blade element velocity
u_a, u_t	Nondimensional axial and tangential components, respectively, of induced velocity from lifting-line calculation based on model or ship velocity
V	Model or ship velocity
$\underline{V}$	Resultant wake velocity vector
V_b	Resultant inflow velocity to blade
$\overline{V}_b$	Mean resultant inflow velocity to blade
V_r	Radial component of velocity vector
$\overline{V}_r$	Mean radial component of velocity vector
V_t	Tangential component of velocity vector
$\overline{V}_t$	Mean tangential component of velocity vector
$(\tilde{V}_t)_n$	n^{th} harmonic amplitude of tangential velocity
V_{tr}	Transverse component of velocity vector
$\overline{V}_v$	Volumetric velocity
V_x	Longitudinal component of velocity vector (normal to the plane of propeller)
$\overline{V}_x$	Mean longitudinal component of velocity vector

$(\tilde{V}_x)_n$	n^{th} harmonic amplitude of longitudinal velocity
$V_{x_{corr}}$	Corrected longitudinal velocity
$\overline{V}_{x_{corr}}$	Mean corrected longitudinal velocity
W_x	Volumetric mean wake coefficient
X,Y,Z	Cartesian coordinates
x	Nondimensional radius r/R (radial coordinate)
x_h	Nondimensional radius at hub
α_h	Projected angle of velocity vector on X-Y plane
α_v	Projected angle of velocity vector on X-Z plane
β	Advance angle in degrees
$\overline{\beta}$	Mean advance angle
$\Delta\beta$	Variation of advance angle from its mean
θ	Position angle (angular coordinate) in degrees

Hull coefficients are in accordance with SNAME recommended standard.

ABSTRACT

This report presents the results of an analysis of the wake of single-screw DE-type ship models using the IBM-7090 Computer. The data presented are the interpolated longitudinal and tangential velocity distributions, their computed mean values, the harmonic contents of these velocity components, the resultant inflow velocity distribution, and the advance angles and their variations. Also included are the calculated volumetric wake velocities.

INTRODUCTION

The problems of propeller cavitation, noise, and vibration have long been matters of great concern to naval architects. During the past decade, the trend of most ship designs has been toward high speed and therefore, high power. As this trend continues, the seriousness of these problems is magnified, and in many instances, they become the primary design considerations, especially for some of the modern naval ships. The source of the problems is attributed, at least partially, to the nonuniform character of the velocity field in which a propeller operates. In order to minimize the serious effect of these phenomena on the life of machinery and equipment and on the performance and the safety of ships, it is essential to know more about the flow pattern behind a ship and its characteristics and to find means to reduce these problems to an acceptable degree.

Because of the complexity of the ship configuration, there exists no theoretical means by which wake behind a ship can be adequately estimated; consequently, naval architects have relied upon experimental methods from which velocities at discrete test points are obtained. In the past, these experimental data could be analyzed only to a limited extent using time-consuming hand computation and curve-fairing techniques. These analyses usually provided information on the magnitude and direction of the velocity at the test points and a map of isovelocity contours.

The advent of the digital computer has revolutionized our concepts and procedures of numerical computation by permitting additional useful

information to be obtained from a more detailed analysis of the experimental data. The first such attempt was made on the wake analysis study conducted on the SSN(N)598-Class submarine.[1] This also opened the possibility that much unassimilated information existed in the numerous three-dimensional wake surveys conducted at the Taylor Model Basin during the past 20 years. These data had originally been analyzed individually for the particular ship design involved. By viewing them as a whole, it was hoped to furnish naval architects and marine engineers with information on the wake characteristics of the various types of hull forms built during the past two decades and so guide future design efforts. With this goal in mind, a research project was initiated by the authors to reanalyze all of the three-dimensional wake surveys conducted at the Model Basin.

Although the information presented is intended primarily to assist the propeller designers in obtaining the best propeller for a given wake field, the comparative quantities among various wake patterns should provide guidance in the choice of hull forms to facilitate the desired propeller performance. Through this work it is hoped that the hull and propeller designers and experimenters can be brought closer together and that each can assist the other in achieving better overall ship designs.

For convenience, the ship models in this project have been grouped into two major catagories, the naval and the merchant types. Each type has been further subdivided into smaller groups by number of propellers, i.e., single screw, twin screw, and quadruple screw. Separate reports on the studies of each group will be issued.

It is the purpose of this, the first report, to:

1. Describe in some detail the methods used in analyzing the wake data.
2. Provide the ship designer with suggested methods for the use of these data in current and future design work.
3. Present the results of the first group of ships analyzed - the single-screw, DE-type naval vessels.

---

[1] References are listed on page 18.

TEST PROCEDURE

The wake surveys for the various models contained in this report were conducted in the deep-water towing tanks at the Model Basin. All were made within the last 10 years, and in general, the technique and instrumentation employed have been the same throughout this period.

To obtain the velocity field behind a ship model, the pressures at various points in the field are measured with a spherical pitot tube while the model is being towed at a given speed and draft condition. From the measured pressures, the dynamic pressures at test points are derived. A typical arrangement of instruments on the model is shown in Figure 1. The rig consists of a pitot tube assembly, a clamping mechanism, a transverse mount, a fore-and-aft mount, a baseplate, and a manometer board. The pitot tube assembly is shaped like the letter "L," a horizontal arm with the spherical head at its end and a vertical post which is clamped to the transverse mount by the clamping mechanism. The transverse mount is attached to the fore-and-aft mount and can be moved in the transverse direction. The fore-and-aft mount is attached to the baseplate and can be moved in the fore-and-aft direction. The baseplate is mounted with the same fore-and-aft angle of inclination as the shaft, i.e., the baseplate is mounted parallel to the shaftline. The clamping mechanism is so designed that the vertical post of the pitot tube assembly can be moved vertically and can also be rotated about the longitudinal and the horizontal axes. The entire rig is so designed that a displacement of the pitot tube at the lower end in the field corresponds to a one-to-one displacement at the upper end. The fore-and-aft mount is used to position the pitot tube in the fore-and-aft direction. When the pitot tube is placed in the desired plane, its movement from point to point in this plane is done by adjusting the vertical and transverse positions of the tube according to a predetermined field target suitably mounted on the stern of the model. A pointer attached to the upper end of the vertical post enables determination of the exact position of the lower end of the pitot tube. The location of the pointer on the target place indicates the corresponding location of the pitot tube in the field.

For the ships reported here, only one-half of the propeller field is surveyed because for a single-screw ship, the flow at the propeller plane is symmetrical with respect to the center vertical axis. For each field point, pressure readings are taken from a manometer board mounted on the towing carriage after a steady-flow condition is established. Usually two to five runs are required for each field point before the manometer readings stabilize to within 0.1 in. of water. For each of the ships, measurements were made at only one speed.

The pitot tubes used for the surveys presented in this report were of similar design, i.e., the so-called five-hold design. This tube has a total of five holes, three in each of the vertical and horizontal planes, one being a common center hole. The construction and calibration of this five-hole tube as well as the test and data analyzing procedures are described in References 2 and 3.

The field points (see Figure 2) in general, were suitably selected in the plane of propeller circumferentially distributed along several radii. Since the surveys were conducted at various times, under different circumstances, and for varying purposes, the lack of uniformity in these tests is to be expected. The selection of field points is no exception. For the surveys reported, the total number of field points range from 21 at three radii to 44 at four radii for one of the latest models, 4954. The angular intervals also vary, and the points are usually not equally spaced for each survey.

REDUCTION OF DATA

All the data presented in this report were reduced from the test data of various surveys with the aid of the IBM-7090 Computer at the Applied Mathematics Laboratory of the Model Basin. Two computer programs were used: "Applied Mathematics Laboratory Problem XF10, Wake Survey Calculations" (AML XF10) and "Applied Mathematics Laboratory Problem 840-219, Wake Analysis" (AML 840-219). The AML XF10 program is used to convert the test data from five readings at each test point into three nondimensional velocity components, which are the ratios of the tangential, longitudinal, and radial

velocities to the model test velocity, in accordance with the instructions outlined in Reference 2. From the output of this program, wake velocity diagrams are made as shown in Figures 5 through 10.

The AML 840-219 program is used for analysis. Briefly, this program incorporates a double interpolating routine by which a given set of values of velocity components at the test points may be interpolated or extrapolated in both the radial and circumferential directions such that values at points other than the test points may be obtained. It also includes an harmonic analysis subroutine which determines the harmonic contents of the interpolated velocity curves in the circumferential direction at desired radii. A discussion of this computer program and instructions for preparation of input data are given in Reference 4.

For this analysis, the test data are reduced in two steps:

Step 1: Computer Fairing of Test Data

Data at the test points are first entered as input to the computer program. The computer interpolates, or extrapolates, the input data and provides the values of the tangential and longitudinal velocity components at various specified angular positions and radii in tabular form. Based on these tables, faired curves of velocity components plotted circumferentially at the various radii in the input are also obtained. These represent computer faired curves of the test data. From these curves, the correctness of input data is checked. These curves also afford us an opportunity to determine whether the test data are reasonable. Should data at some points be found, in our judgement, not too plausible, then these data are modified. Also, at positions where there are large fluctuations in velocities, additional input data obtained from hand-faired curves are entered in subsequent computations.

Step 2: Final Computation

When the above modifications are necessary, a second computer run is made. From this computation, revised tables of the tangential and longitudinal velocities components are obtained which enable us to map the entire velocity field in the wake. Also obtained are the following computed quantities at

specified advance coefficients J_a according to the expressions given below (see Figure 3):

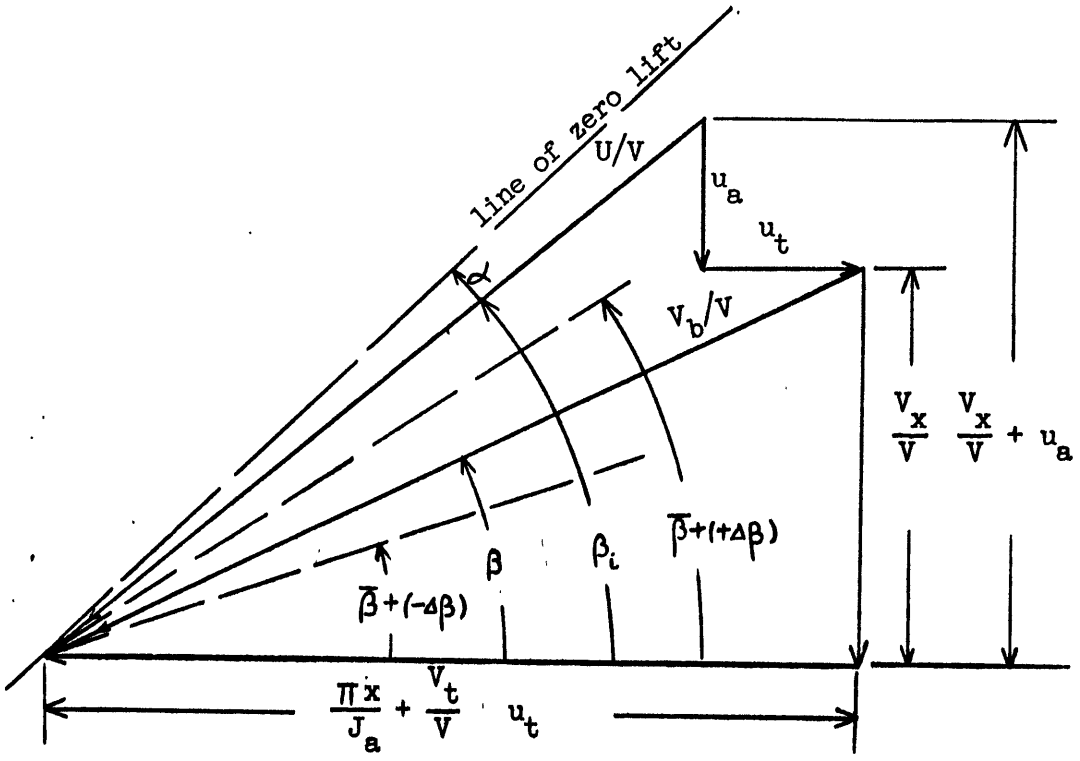

Figure 3 - Velocity Diagram

a. Resultant inflow velocity to propeller blade squared V_b^2

$$(V_b(x, \theta)/V)^2 = (V_x(x, \theta)/V)^2 + (\pi x/J_a + \dot{V}_t(x, \theta)/V)^2 \qquad [1]$$

where x is the nondimensional radius,

θ is the position angle,

V_x is the longitudinal velocity,

V_t is the tangential velocity, and

V is the test model speed.

b. Advance angle β

$$\beta(x, \theta) = \tan^{-1}\left[(V_x(x, \theta)/V) \,/\, (\pi x/J_a + V_t(x, \theta)/V) \right] \qquad [2]$$

c. Corrected longitudinal velocity components $V_{x_{corr}}$

$$V_{x_{corr}}(x, \theta) = V_x(x, \theta) - V_t(x, \theta) \tan\beta(x, \theta) \qquad [3]$$

This is a fictitious or pseudo-longitudinal velocity. When used in conjunction with an assumed zero tangential velocity, it gives the same advance angle as would be obtained from the actual tangential and the longitudinal velocities. This pseudo-longitudinal velocity may be used for simulating the flow field, taking into account the effect of the tangential component. It should be noted from the following diagrams with this correction that the resultant velocity V_b is not quite correct, but the maintenance of the proper advance angle at all angular positions is an improvement over the one without this correction for the tangential velocity.

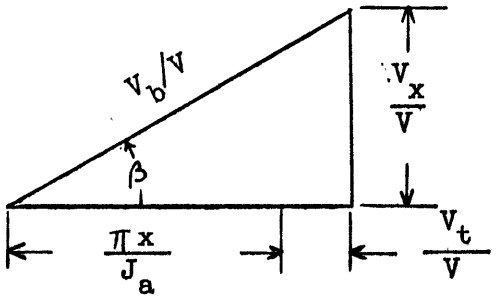

Actual

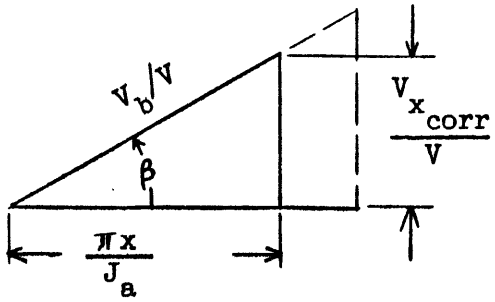

Corrected

For the data reported here, the ranges of the output radii x specified are from 0.3 to 1.0 at 0.1 intervals, and the ranges of the angular positions θ are from 0 to 360 deg (the starboard half, 180 to 360 deg, is a mirror image of the port half, 0 to 180 deg) at 2.5-deg intervals.

The above tables of $\frac{V_x}{V}$, $\frac{V_t}{V}$, $(\frac{V_b}{V})^2$, β, and $\frac{V_{x_{corr}}}{V}$ are analyzed for their harmonic contents in the circumferential direction at various

specified radii using a harmonic analysis subroutine from which the amplitudes and phase angles for various harmonics and the circumferential mean values are obtained.

Also computed at each radius are the following:

d. Volumetric velocity $\bar{V}_v$

$$\bar{V}_v(x)/V = 2 \int_{x_h}^{x} x \, (\bar{V}_{x_{corr}}(x)/V)dx \qquad [4]$$

where $\bar{V}_v$ has a dimension of volume per unit time, and $\bar{V}_{x_{corr}}$ denotes the mean value of $V_{x_{corr}}$.

e. Volumetric mean wake velocity $1-W_x$

$$1-W_x(x) = (\bar{V}_v(x)/V) \; / \; \pi (x^2 - x_h^2) \qquad [5]$$

where W_x is a volumetric mean wake coefficient, and x_h is the radius at propeller hub.

f. Maximum variation in advance angle $\Delta\beta$

$$+\Delta\beta(x) = \beta_{max}(x) - \bar{\beta}(x)$$

$$-\Delta\beta(x) = \beta_{min}(x) - \bar{\beta}(x) \qquad [6]$$

where $\bar{\beta}$ denotes the mean value of β and is defined

$$\bar{\beta} = \tan^{-1}\left[(\bar{V}_x/V) \; / \; (\pi x/J_a + \bar{V}_t/V) \right]$$

where $\bar{V}_x$ and $\bar{V}_t$ denote the mean value of the longitudinal and tangential velocity components, respectively.

g. Pressure factor P

$$P = (V_b^2)_{max} \; / \; \overline{V_b^2} - 1 \qquad [7]$$

This pressure factor reflects the maximum fluctuation in the resultant inflow velocity to the propeller element.

For typical detailed computer output, see results for Model 4954, Reference 5.

PRESENTATION OF DATA

APPLICATION OF WAKE DATA IN PROPELLER-SHIP DESIGNS

Before proceeding with the presentation of the results of the single-screw, DE-type naval ships, we shall briefly discuss some of the ways in which the data obtained from the wake analyses might be used by ship and propeller designers.

In order to achieve a good propeller design, the designer is interested in determining a number of quantities. Of these, the most important are the considerations of performance, possible cavitation and vibration problems, and strength. The use of the wake data in providing quantitative information for each of these items will be discussed briefly as follows:

Performance: A propeller designer is required to design a propeller that will develop a certain thrust or torque for a given set of operating conditions with the highest performance obtainable. In order to accomplish this, he may base his design upon open-water performance, or he may take a more realistic approach and design a wake-adapted propeller, knowing that the velocity field will not be uniform when in service. If the latter course is taken, then information on the wake distribution will be essential to this task. From the velocity survey, the mean values at various radii are obtained, thus providing the propeller designer with the radial distribution of the circumferential mean velocity for the wake-adapted propeller design.

Cavitation: Another consideration in propeller design is the cavitation problem. Cavitation is known to be caused by unfavorable pressure distribution over the propeller blades. In order to minimize this problem, efforts are usually made to ensure a desirable pressure distribution by properly choosing the load distribution, blade geometry, etc. It is also known that

the unsteadiness of the wake field in which a propeller operates has considerable effect on the cavitation characteristics of a propeller. In general, propeller blade sections have incipient cavitation characteristics of the type shown in the following diagram (e.g., see Reference 6).

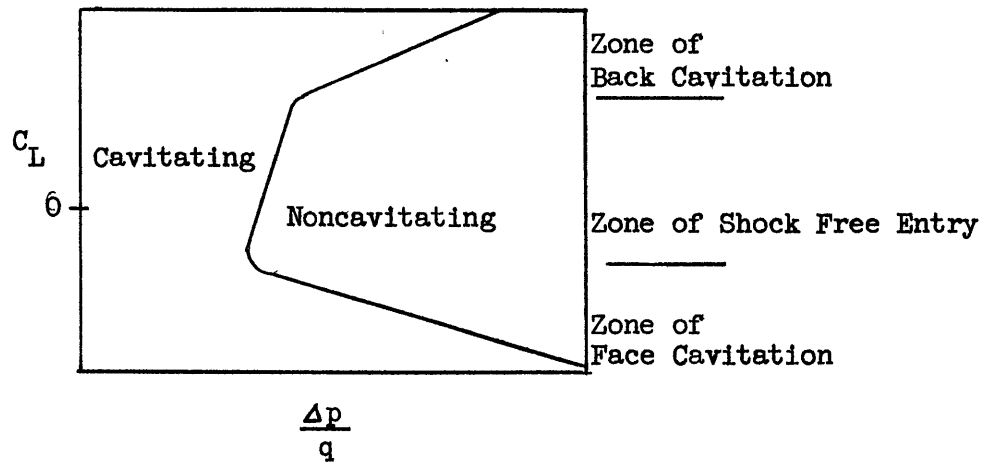

This diagram shows that the inception of cavitation is related to the section lift coefficient C_L and to the pressure coefficient $\frac{\Delta p}{q}$. Since the lift coefficient is a function of α and the pressure coefficient is a function of the square of the blade-element velocity U, cavitation is a function of the angle of attack α and the blade-element velocity U. It can be seen from the propeller blade-element velocity diagram (Figure 3) that α and U are related to the magnitude of the wake velocity. An adequate knowledge of the wake velocity distribution is therefore essential to the appraisal of the cavitation problem of the propeller operating in wake. This is a rather complex unsteady propeller problem. The computational techniques for the unsteady problem are presently being developed and are not yet available; one can make only a rough estimate by the use of the quasi-steady technique. However, if one is interested only in obtaining information on the cavitation characteristics of various wake patterns, he may compare some of the computed wake data of the various patterns and make a sound judgement as to which pattern is least objectionable from the standpoint of inciting cavitation.

An inspection of the velocity diagram (Figure 3) indicates that the hydrodynamic pitch angle β_i decreases or increases as the advance angle decreases or increases, albeit in a complex relationship. Correspondingly, the angle of attack α varies with the change in advance angle. By a similar process of analysis, it can be shown that the blade-element velocity U varies directly with the resultant inflow velocity V_b. Consequently, we may relate the blade-element pressure coefficient to V_b^2 which can be computed from the wake data at a given value of the advance coefficient J_a. To facilitate the comparison of various model data, we define the maximum variations in the advance angle from its mean $\Delta\beta$ as in Equation [6]. Loosely speaking, a large $\Delta\beta$ indicates a possible large variation in angle of attack. Also defined is a pressure factor P, as in Equation [7], which represents the maximum fluctuation in the resultant inflow velocity squared from its mean, or roughly the maximum reduction in the pressure coefficient. The maximum variation in the advance angle and the pressure factor computed for the various wake patterns may be compared for their relative effectiveness in minimizing the cavitation problem.

Another use of wake data is in the area of cavitation testing in the variable-pressure water tunnels. McCarthy[7] developed a method of simulating a flow field to have longitudinal velocity components as prescribed by the use of screens placed upstream of the propeller. Using this technique and based on the data obtained from the wake analysis, it is now possible to duplicate approximately the flow field behind a given ship design in the water tunnels for testing of propellers on a more realistic basis.

Vibration: Equally significant is the vibration problem caused by the alternating forces generated by the propeller. When a propeller operates in a nonuniform flow field, the lift generated at any instant of time by each of the blades is not equal. Consequently, as the propeller rotates in the field, the thrust and torque are time dependent and are cyclic in character. As a result of this phenomenon, serious vibration may exist in the shafting system which can be transmitted to the hull through the bearings or machinery foundations. It is therefore desirable to be able to appraise

the possible vibration problem by estimating the magnitude of the vibratory forces produced by a given propeller design in a particular wake field. Various theories and computational methods have been developed for this purpose. The results from the calculations along with model experiments should provide adequate information for evaluating the extent of this problem for a particular ship-propeller design. Before this stage is reached, however, it is possible to use the results of a harmonic analysis of the circumferential velocity distributions to provide information on the comparative strengths and radial distributions of the various harmonics in a given wake as well as a comparison of the strengths of the harmonics in different wake patterns. This information can guide the propeller designer in his choice of number propeller blades and the possible skew desired for the preliminary designs. It can also assist the hull designer to select a stern hull form which has weaker harmonics for the type of propeller under consideration.

Some investigators, e.g., Rütger and Breslin,[8] who have developed theories of propeller action in a nonuniform flow field have shown that the magnitudes of the unsteady thrust and torque are determined for all practical purposes by the harmonics in the wake which coincide with the number of propeller blades and their integer multiples, i.e., a five-bladed propeller will respond to the fifth, tenth, fifteenth, wake harmonics, etc. Correspondingly, the magnitude of the bending moments and the transverse forces respond to the two wake harmonics adjacent to the number of propeller blades and the integer multiples of the propeller blades; i.e., a five-bladed propeller will respond to a fourth-sixth, ninth-eleventh, fourteenth-sixteenth harmonics of the wake and so forth.

Strength: A propeller should be designed to have adequate strength to withstand the stress that is imposed by the loading on the blades. In practice, the maximum thickness at blade sections is usually calculated by using certain formulas based upon the designed load with some factor of safety included. Since the propeller most probably will operate in a nonuniform flow field, the loading will be somewhat different from the designed value due to the change in angle of attack. It is also desirable to assess

the maximum fluctuation in loading by estimating the maximum change of angle of attack from the wake data for a given wake pattern. As discussed previously in the paragraph on cavitation, this may be calculated using the quasi-steady technique. Again, if one is interested only in the comparative merits of various wake patterns, then the comparative values of fluctuation in the advance angle for these patterns may be indicative of comparative maximum loading fluctuations.

RESULTS OF ANALYSES

The six models reported here are of similar hull form with the obvious exception that four of the models have large sonar domes at the bow (see Figure 4). The various hull parameters are comparable (Table 1), the variation in the significant hull coefficients being about ± 5 percent. With the exception of the rudder, the stern appendages are similar on all six models. When the tests were conducted, all appendages were installed except the rudder. The models were tested at comparable speeds.

Two types of information are presented: the test data and the computed results. The test data are those obtained from the model experiments at the discrete test points. The computed data are those quantities calculated on the basis of the test data. For convenience, a standard length of 400 ft, a standard propeller diameter of 16 ft, and a standard speed of 27.4 knots ($V/\sqrt{L} = 1.37$) were chosen for the presentation of the computed results.

The test data are presented in Figures 5 through 10. Also shown are the transverse velocity vectors in the plane of the propeller at the various test points. The body plan in the proximity of the propeller plan and the propeller shaft struts are alos shown in these figures.

Figures 11 through 16 show the interpolated circumferential distributions of the longitudinal and tangential velocity components at the test radii. The nondimensionalized radii are those of the model propeller designed for the ship. Where the faired curves do not pass through the test points, the data are considered in question. The distribution curves for the various models look very much alike. All the longitudinal values show a dip near 0-deg angular points which arises from the shadow of the propeller shaft.

The tangential wake shows an almost sinusoidal curve of shaft frequency; this is due to the angularity of the propeller shaft to the flow. In this series of tests, measurements behind the strut have been noted to be erratic. In order to estimate the effect of struts on the longitudinal wake velocity in the plane of the propeller, calculations have been made based on Reference 9 for the strut arrangement of Model 4954 (Figure 16), assuming that the flow was along the longitudinal axis of the strut chord. The calculation shows that the wake band behind a strut of the size used in this model will be smaller than the diameter of the pitot tube head; thus accurate velocity measurements are not possible. Therefore, in analyzing the data, the faired values are used. The computed results have also been plotted in Figure 16. As may be noted, the velocity defect behind the strut is relatively small. The effect of struts has not been introduced into the wake computations for Model 4954.

The circumferential distributions of the longitudinal and tangential velocity components are analyzed for their harmonic contents from which the circumferential mean values are obtained. Due to the symmetry about the center vertical plane of this group of models, the circumferential mean of the tangential velocity is zero. The circumferential mean longitudinal velocities at various radii are plotted in Figure 17. The exceptionally good agreement among the various models is due to the fact that the circumferential distributions of the velocity components are similar as remarked above; this enables us to draw a single curve to represent the models studied. Also shown in Figure 17 are the calculated dimensionless volumetric velocity and the volumetric mean velocity distributions.

The calculated amplitudes of the first (shaft frequency) and the fourth through seventh harmonics are shown in Figure 18. A negative amplitude in the fourth through seventh harmonics indicates that it is out of phase with the first harmonic by 180 deg. We observe that the amplitude of the first harmonic is considerably larger than those of the higher harmonics. For the higher harmonics, the scale is enlarged to show the scatter of the values for the various models. The curves shown are drawn for Model 4954 because

considerably more test data were available on this model to define the circumferential variations, particularly in the shadow of the shaft which has a large influence on the higher shaft frequency harmonics. In general, one may expect that the amplitude decreases as the number of harmonics increase, as shown here. The fact that the calculated values do show large scatter indicates that they are sensitive to the shape of distribution curves analyzed. Large hollows and humps in the curves may not affect the mean value very much, but they certainly will affect the harmonic contents of the curve.

For the purpose of furnishing useful information in analyzing the performance and the cavitation characteristics of a propeller due to nonuniform wake, the wake data are further analyzed in terms of maximum variations, or fluctuations in the resultant inflow velocities to the propeller blade and in the advance angles.

As shown in Figure 3, the velocity at the blade element depends on the propeller rotational speed. In order to establish proper geometric relationships, it is necessary to assume certain operating conditions, namely the advance coefficient J_a. Since the designed advance coefficients for the various models vary from 0.722 to 0.846, an advance coefficient of 0.8 was arbitrarily chosen for these computations.

The calculated mean values of the advance angle at various radii are shown in Figure 19, together with the maximum variations. Again, due to the close agreement in the computed results, the various models are represented by single curves. This means that the advance angle may be anywhere within the band bonded by $\bar{\beta} + (+\Delta\beta)$ and $\bar{\beta} + (-\Delta\beta)$ curves in a quasi-steady sense. On the same figure are also shown the so-called pressure factors as defined by Equation [7]. This quantity represents the minimum pressure at the propeller blade element resulting from the variations in the inflow velocity expressed as percent of the mean resultant velocity. Since the variations in the advance angles and the pressure factors are dependent upon the value of the advance coefficient J_a, computations of these quantities for a range of values of J_a from 0.6 to 1.0 are made, and the results are shown in Figure 20. These curves indicate that the variations are relatively insensitiv to the values of J_a.

It should be noted that the variations in advance angles are affected largely by the circumferential distribution of the longitudinal velocity while the pressure factors are influenced chiefly by the tangential velocity for the range of mean advance angles shown in Figure 19.

CONCLUSIONS AND RECOMMENDATIONS

1. As mentioned previously, four of the six models have sonar domes at the bow. Two of these models, 4881 and 4870, have domes of different designs; otherwise they are identical. Inasmuch as the data for these two models show excellent agreement and the results of all six models do not reflect the effect of these domes, it is concluded that the presence of the sonar domes or, more generally, the variation in the designs of the forebody, has very little or no effect on the stern wake. This means that the wake distribution is affected primarily by the stern hull and appendage configuration.

2. It would appear from the wake calculations that struts about 2 chord lengths upstream on these models have almost negligible effect upon the wake in the plane of the propeller, at least in the outer portion of the propeller disk where the measurements were made.

3. In view of the good agreement for the various models with similar stern configurations, it will not be too farfetched to conclude that we may expect a similar wake pattern for models with a stern configuration similar to the ones studied here. Any future experimental work should be concentrated upon more carefully delineating the velocity pattern in the shadow of the propeller shaft. This would permit more accurate determination of the magnitude of the propeller blade frequency and higher harmonics. Tests at other speeds would assist in determining if the wave effect upon the velocity pattern was very significant.

4. For all practical purposes, the mean nondimensional longitudinal velocity and the volumetric mean wake velocity are linearly distributed along the radius with 1.01 at $r/R = 0.3$ and 0.98 at $r/R = 1.0$ for the circumferential mean longitudinal velocity, and 1.03 at $r/R = 0.3$ and 0.99 at $r/R = 1.0$ for the volumetric mean wake velocity.

5. The positive and negative variations in the advance angle from the mean are of about equal magnitude, varying from 5 deg at the most to less than 1 deg at the tip of the propeller. The maximum fluctuations in the resultant inflow velocity in terms of the mean values are in the order of 20 percent at the hub and diminish to 7 percent at the tip of the propeller.

As a result of this analysis, the following recommendations are made regarding future work on the DE-type ships.

1. Any future wake surveys conducted on ship models of this type should include a more careful exploration in the region behind the propeller shaft. This should be made on both sides of the centerline of the model as there is evidence from other work to indicate that there is not complete symmetry of flow in the propeller plane due to inaccuracies in model construction or velocity measurement.

2. If it should be desirable to increase the length of the skeg, the effect on vibration and cavitation performance can easily be estimated by careful survey of the top center portion of the propeller disk.

3. The effect of the ship wave train at different speeds upon the wake performance at two speed conditions may be important. This effect can be examined by testing at another speed.

4. The results of this analysis may be used directly for propeller design purposes on future DE designs with hull characteristics and a design speed similar to those contained in this report.

5. Although the wake survey and the estimate from NACA experiments suggest that well-placed struts would have negligible effects on cavitation and vibration, the effect of struts should be investigated further by studies in a variable-pressure water tunnel and vibration experiments on a ship model.

ACKNOWLEDGMENTS

The authors wish to express their thanks to Max H. Morris, Inc., especially to Mrs. Ruth Goldberg, for assistance in the collection of data and in the preparation of final graphs and to Mr. George Smith of the Applied Mathematics Laboratory for his help in the computer work.

REFERENCES

1. Hadler, J.B. and Wermter, R., "Comparison of Wake Parameters of Various Modified Hull Forms of SSB(N)598 Class Submarines," David Taylor Model Basin Report C-1390 (Jun 1962, Preliminary Copy), CONFIDENTIAL.

2. Pien, P.C., "Five-Hole Spherical Pitot Tube," David Taylor Model Basin Report 1229 (May 1958).

3. Stuntz, G.S., et al, "Series 60 - The Effect of Variation in Afterbody Shape Upon Resistance, Power, Wake Distribution, and Propeller Excited Vibratory Forces," Transactions of the Society of Naval Architects and Marine Engineers, Vol. 69 (1961).

4. Cheng, H. M., "Analysis of Wake Survey of Ship Model, Computer Program, AML Problem No. 840-219F," David Taylor Model Basin Report 1804 (Mar 1964).

5. Weaver, A.H. Jr., and Hubble, E.N., "Powering Characteristics, Appendage Orientation, Flow Studies, and Wake Survey for a DE (Ocean Escort) Represented by Model 4954," David Taylor Model Basin Report C-1658 (Nov 1963) CONFIDENTIAL.

6. Van Lammeren, W.P.A., "Resistance, Propulsion and Steering of Ships," The Technical Publishing Company H. Stam-Haarlem-Holland (1948), p. 163.

7. McCarthy, J., "A Method of Wake Prediction in Water Tunnels," David Taylor Model Basin Report 1785 (Oct 1963).

8. Ritger, P. D. and Breslin, J.P., "A Theory for the Quasi-Steady and Unsteady Thrust and Torque of a Propeller in a Ship Wake," Stevens Institute of Technology Experimental Towing Tank Report 686 (Jul 1958).

9. Silverstein, A., et al, "Downwind and Wake Behind Plain and Flapper Airfoils," National Advisory Committee for Aeronautics Report 651 (1939).

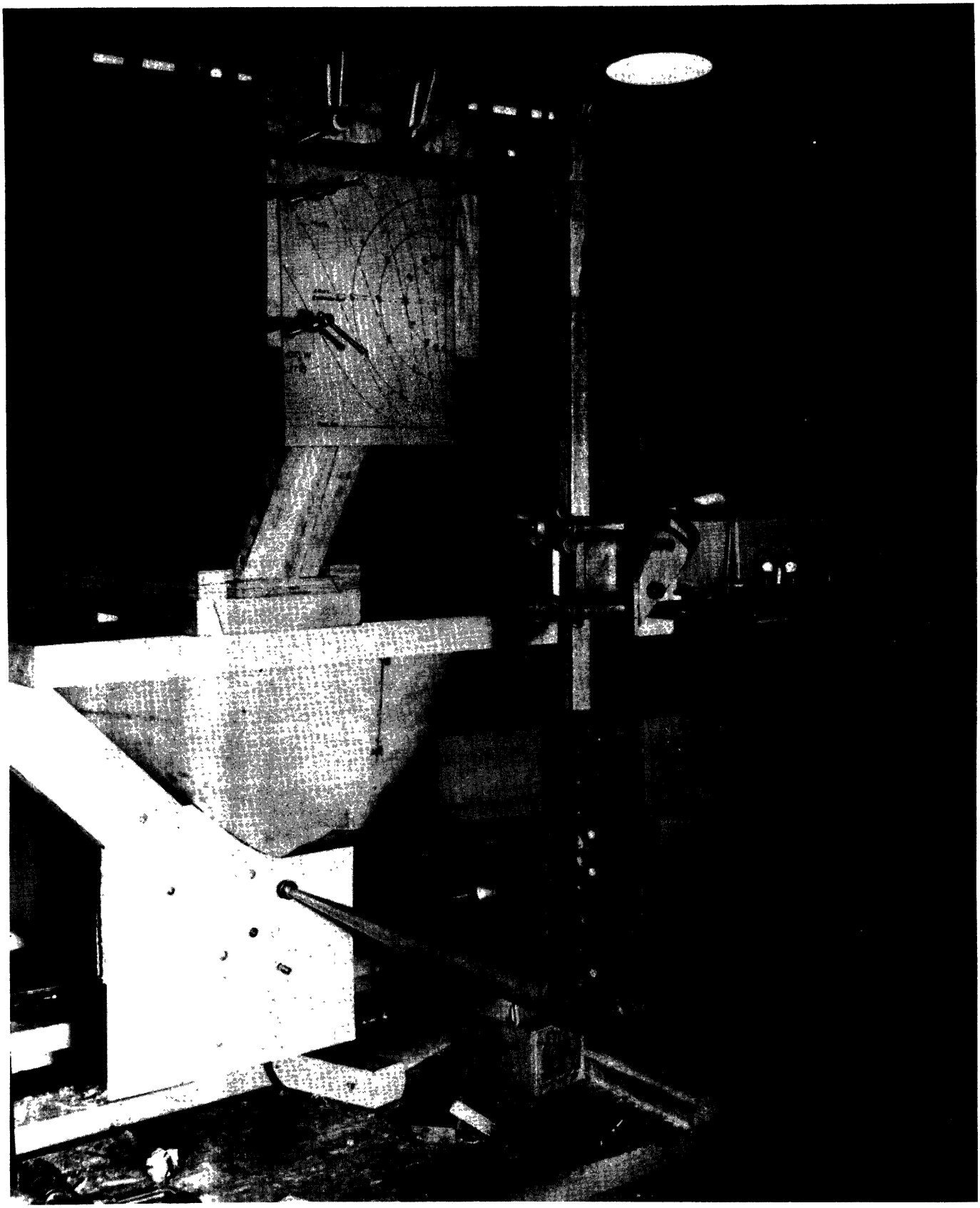

NP-21-46759

Figure 1 - Arrangement of Pitot Tube Assembly

TABLE 1

Model Data

Particulars	Model 4360	Model 4554	Model 4773	Model 4870	Model 4881	Model 4954
Length on LWL, L_{WL}, ft	18.18	22.22	20.66	19.98	19.98	20.21
Beam B, ft	2.16	2.78	2.38	2.24	2.24	2.28
Draft H, ft	0.703	0.890	0.797	0.743	0.743	0.726
Displacement FW, ton	0.378	0.680	0.536	0.452	0.452	0.451
Test Velocity V, knots	5.83	5.98	6.32	6.11	6.11	6.11
LCB/L_{WL} aft of FP		0.510	0.510	0.493	0.486	0.490
$V/\sqrt{L_{WL}}$	1.37	1.27	1.39	1.37	1.37	1.36
Propeller Diameter D, ft	0.739	0.775	0.739	0.737	0.737	0.768
Advance Coeff. $J_a = V/nD$	0.846	0.722	0.775	0.826	0.830	0.826
LWL Coefficients						
C_B	0.492	0.450	0.492	0.483	0.489	0.485
C_P	0.601	0.560	0.622	0.608	0.616	0.589
C_x	0.818	0.790	0.791	0.794	0.794	0.824
C_{PA}	0.65	0.60	0.67	0.62	0.62	0.60
C_{PVA}		0.61	0.56	0.55	0.55	0.57
L_R/L_{WL}	0.43	0.45	0.45	0.46	0.46	0.47
L_{WL}/B	8.42	8.00	8.66	8.92	8.92	8.86
B/H	3.07	3.12	2.99	3.01	3.01	3.13
$\Delta_{sw}/(.01\ L_{WL})^3$	64.7	64.1	62.5	57.5	58.2	56.3

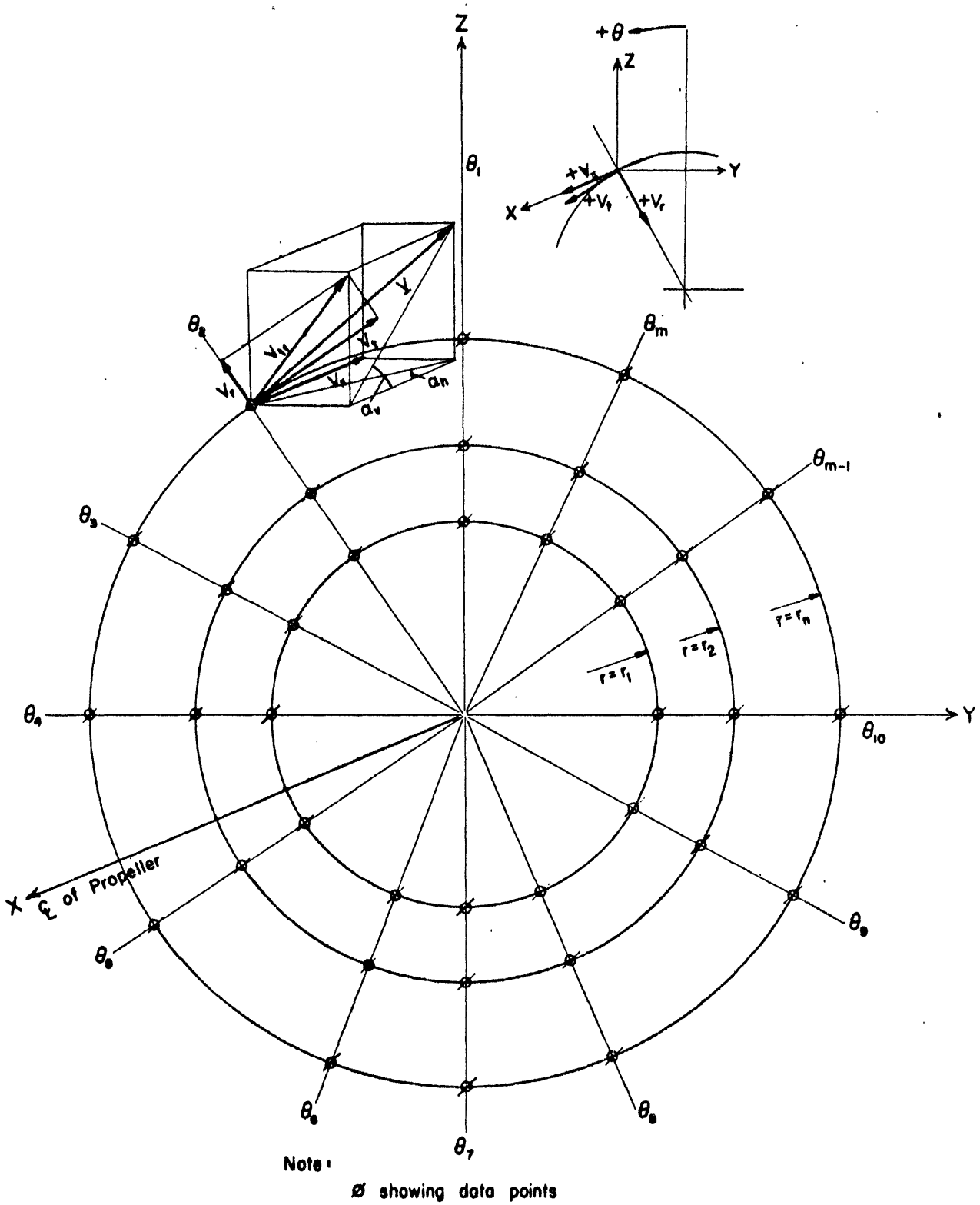

Looking Forward

Figure 2 - Coordinate System of Velocity Components

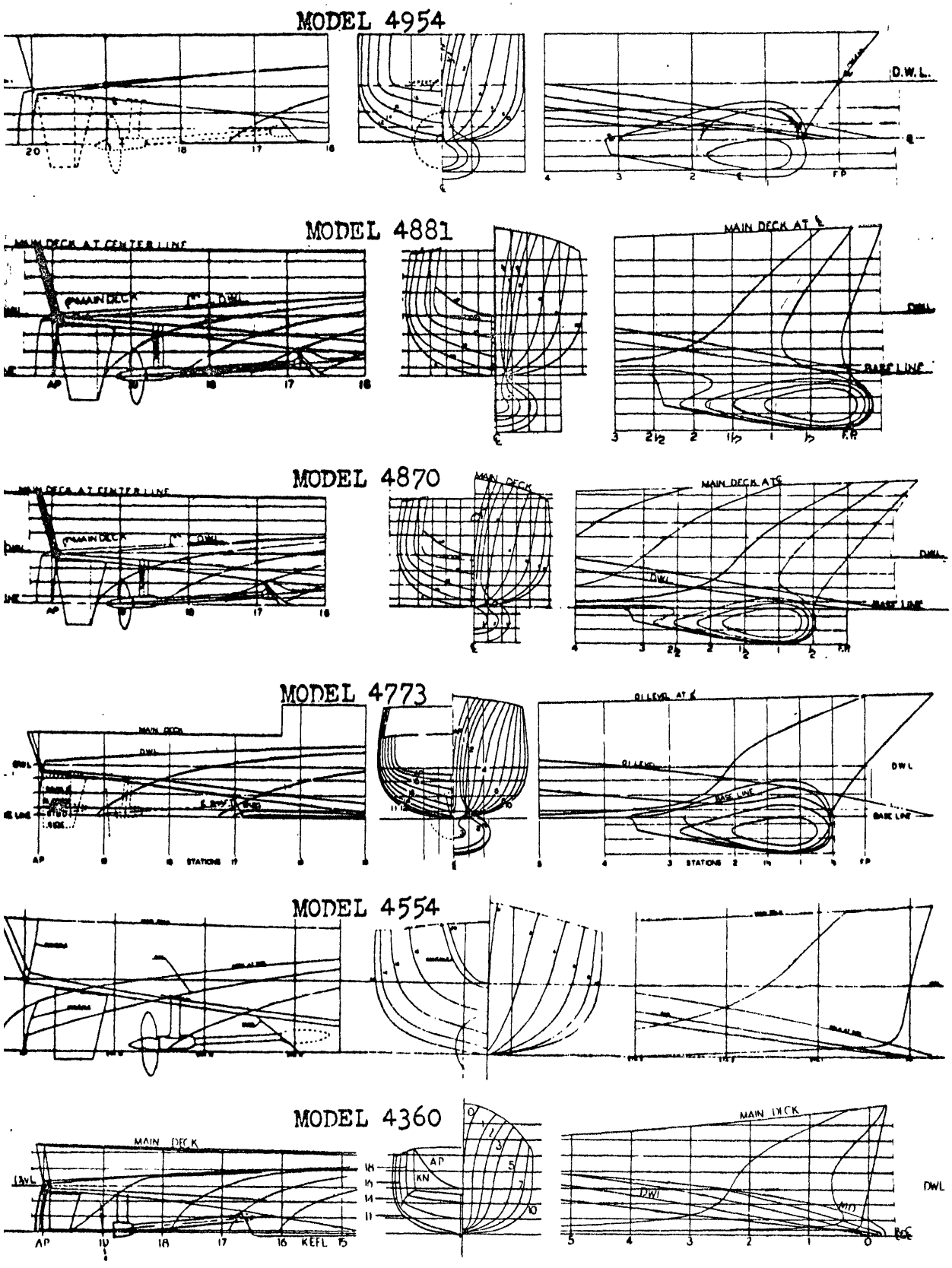

Figure 4 - Lines of Single-Screw, DE-Type Ships

VELOCITY SURVEY IN WAY OF THE PROPELLER
SINGLE SCREW SHIPS
DE TYPE
MODEL 4360-1
MODEL DIMENSIONS
LENGTH (LWL) 18.18 FT
BEAM 2.16 FT
DRAFT .703 FT
DISPLACEMENT .378 TONS F.W.
PROPELLER DIAMETER .739 FT
SPEED 5.83 KT
TEST 19
NOVEMBER 1955

r/R IS THE DISTANCE FROM THE PROPELLER AXIS (r) EXPRESSED AS A RATIO OF THE PROPELLER AXIS (R).

θ IS THE ANGLE MEASURED FROM THE TOP OF THE PROPELLER DISK IN A COUNTERCLOCKWISE DIRECTION.

V IS THE SHIP SPEED.

V_x IS THE LONGITUDINAL (NORMAL TO THE PLANE OF SURVEY) COMPONENT OF THE WATER VELOCITY AND IS POSITIVE IN THE ASTERN DIRECTION

V_t IS THE TANGENTIAL COMPONENT OF THE WATER VELOCITY AND IS POSITIVE IN THE COUNTERCLOCKWISE DIRECTION

V_r IS THE RADIAL COMPONENT OF THE WATER VELOCITY AND IS POSITIVE TOWARD THE SHAFT CENTERLINE.

V_{tr} IS THE TRANSVERSE COMPONENT OF THE WATER VELOCITY AND IS THE VECTOR SUM OF V_t and V_r.

THE VECTOR SHOWN IN THE DIAGRAM IS IN THE DIRECTION OF V_{tr} WITH A MAGNITUDE EQUAL TO V_{tr}/V.

THE VELOCITY MEASUREMENTS WERE MADE IN A PLANE WHICH IS PERPENDICULAR TO THE CENTERLINE OF THE PROPELLER SHAFT AND INTERSECTS THE SHAFT LINE AT STA 19.

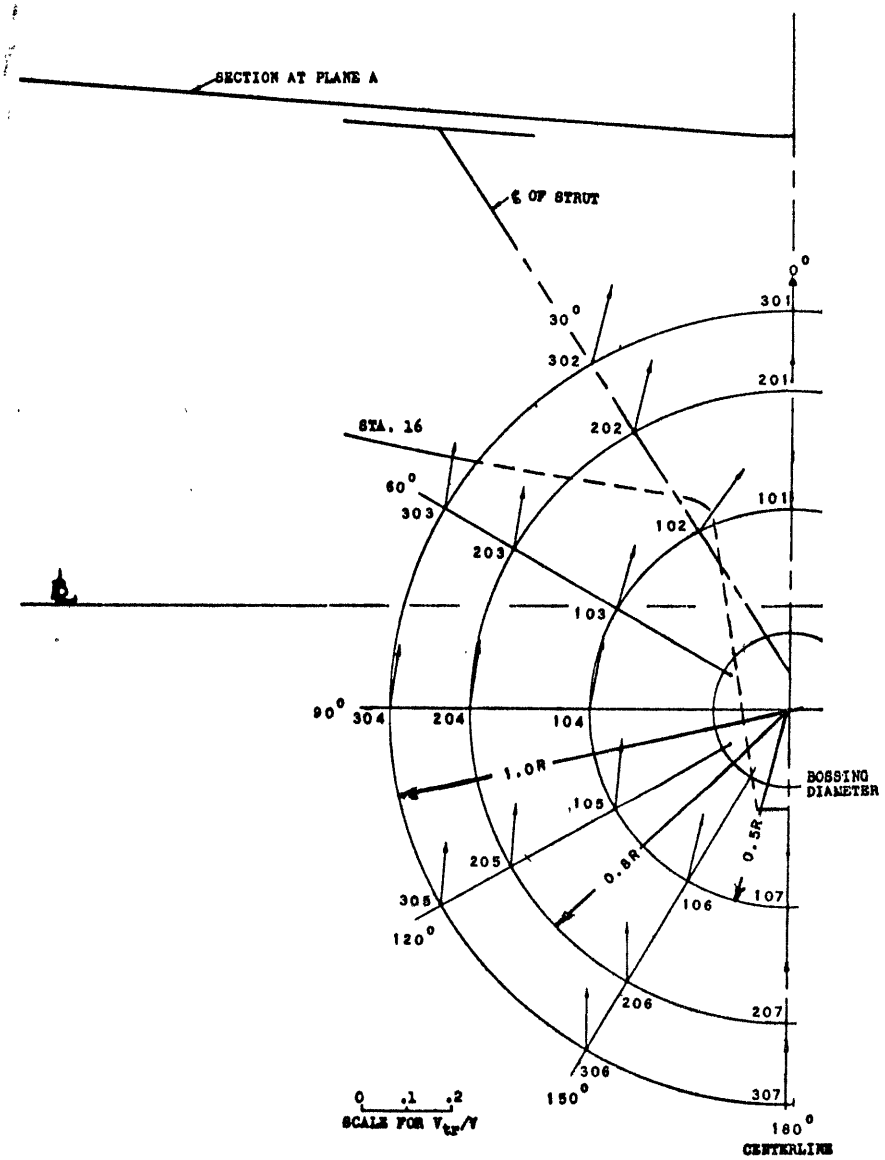

TABLE OF COMPONENT RATIOS

POSITION NUMBER	V_x/V	V_t/V	V_r/V
101	0.92	0	-0.04
102	0.97	-0.16	-0.08
103	1.02	-0.14	-0.04
104	1.01	-0.16	0.03
105	1.03	-0.13	0.09
106	1.01	-0.07	0.12
107	1.00	0	0.14
201	0.96	0	-0.08
202	0.92	-0.12	-0.12
203	1.02	-0.13	-0.05
204	1.01	-0.15	0.02
205	1.01	-0.12	0.08
206	1.01	-0.07	0.12
207	1.00	0	0.14
301	0.91	0	-0.10
302	0.88	-0.13	-0.13
303	1.01	-0.14	-0.06
304	1.01	-0.14	0.02
305	1.01	-0.12	0.08
306	1.03	-0.05	0.15
307	1.03	0	0.14

Figure 5 - Wake Velocity Diagram and Test Data, Model 4360

VELOCITY SURVEY IN WAY OF THE PROPELLER
SINGLE SCREW SHIPS
DE TYPE
MODEL 4554

MODEL DIMENSIONS	
LENGTH (LWL)	32.23 FT
BEAM	3.78 FT
DRAFT	.890 FT
DISPLACEMENT	680 TONS F.W.
PROPELLER DIAMETER	.775 FT
SPEED	5.98 KT

TEST 10
SEPTEMBER 1955

r/R IS THE DISTANCE FROM THE PROPELLER AXIS (r) EXPRESSED AS A RATIO OF THE PROPELLER AXIS (R).

θ IS THE ANGLE MEASURED FROM THE TOP OF THE PROPELLER DISK IN A COUNTERCLOCKWISE DIRECTION.

V IS THE SHIP SPEED

V_x IS THE LONGITUDINAL (NORMAL TO THE PLANE OF SURVEY) COMPONENT OF THE WATER VELOCITY AND IS POSITIVE IN THE ASTERN DIRECTION.

V_t IS THE TANGENTIAL COMPONENT OF THE WATER VELOCITY AND IS POSITIVE IN THE COUNTERCLOCKWISE DIRECTION

V_r IS THE RADIAL COMPONENT OF THE WATER VELOCITY AND IS POSITIVE TOWARD THE SHAFT CENTERLINE.

V_{tr} IS THE TRANSVERSE COMPONENT OF THE WATER VELOCITY AND IS THE VECTOR SUM OF V_t and V_r.

THE VECTOR SHOWN IN THE DIAGRAM IS IN THE DIRECTION OF V_{tr} WITH A MAGNITUDE EQUAL TO V_{tr} V.

THE VELOCITY MEASUREMENTS WERE MADE IN A PLANE WHICH IS PERPENDICULAR TO THE CENTERLINE OF THE PROPELLER SHAFT AND CENTERLINE OF PROPELLER IS 280 FT FROM F.P

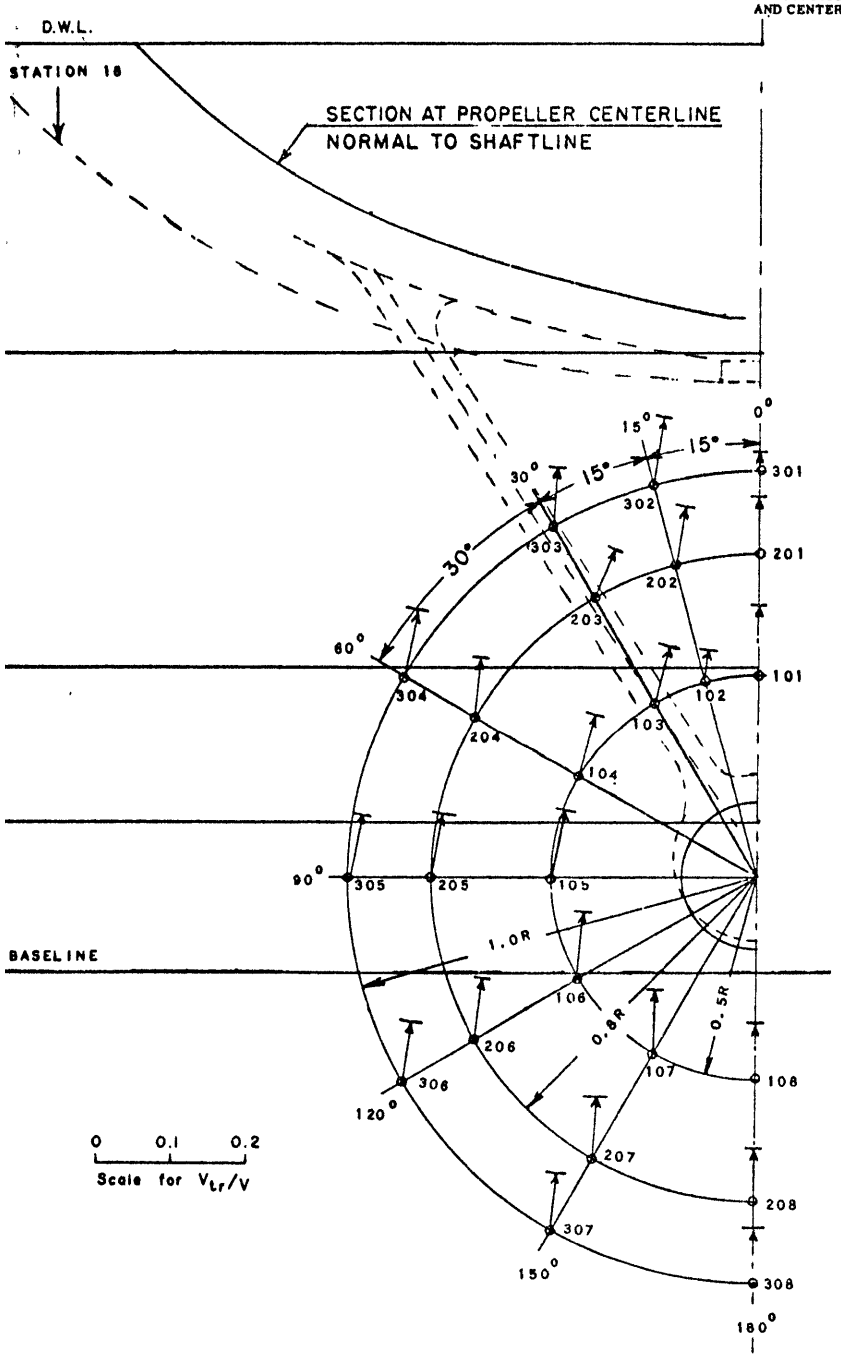

TABLE OF COMPONENT RATIOS

POSITION NUMBER	V_x V	V_t V	V_r V
101	0 998	0	-0. 164
102	0 984	-0 060	-0. 143
103	0. 934	-0 091	-0. 095
104	1. 007	-0 146	-0. 041
105	1 014	-0 161	0. 026
106	1 016	-0. 128	0 087
107	1. 016	-0. 043	0 100
108	1 017	0	0. 129
201	0 968	0	-0 131
202	1. 006	-0. 060	-0 122
203	0. 911	-0. 096	-0 070
204	0 992	-0. 145	-0 062
205	1 008	-0. 149	-0. 062
206	1 009	-0. 113	0. 026
207	1 011	-0 158	0 087
208	1. 009	0	0 121
301	0 909	0	-0 022
302	0. 992	-0 063	-0 143
303	0 896	-0 073	-0 120
304	0. 973	-0. 148	-0. 066
305	1 005	-0. 144	0 026
306	1 001	-0 107	0. 085
307	1. 003	-0. 054	0. 119
308	1 005	0	0 133

Figure 6 - Wake Velocity Diagram and Test Data, Model 4554

VELOCITY SURVEY IN WAY OF THE PROPELLER
SINGLE SCREW SHIPS
DE TYPE
MODEL 4773
MODEL DIMENSIONS
LENGTH (LWL) 20.66 FT
BEAM 2.38 FT
DRAFT .787 FT
DISPLACEMENT .836 TONS F.W.
PROPELLER DIAMETER .739 FT
SPEED 6.32 KT
TEST 10
FEBRUARY 1960

r/R IS THE DISTANCE FROM THE PROPELLER AXIS (r) EXPRESSED AS A RATIO OF THE PROPELLER AXIS (R).

θ IS THE ANGLE MEASURED FROM THE TOP OF THE PROPELLER DISK IN A COUNTERCLOCKWISE DIRECTION.

V IS THE SHIP SPEED.

V_x IS THE LONGITUDINAL (NORMAL TO THE PLANE OF SURVEY) COMPONENT OF THE WATER VELOCITY AND IS POSITIVE IN THE ASTERN DIRECTION.

V_t IS THE TANGENTIAL COMPONENT OF THE WATER VELOCITY AND IS POSITIVE IN THE COUNTERCLOCKWISE DIRECTION.

V_r IS THE RADIAL COMPONENT OF THE WATER VELOCITY AND IS POSITIVE TOWARD THE SHAFT CENTERLINE.

V_{tr} IS THE TRANSVERSE COMPONENT OF THE WATER VELOCITY AND IS THE VECTOR SUM OF V_t and V_r.

THE VECTOR SHOWN IN THE DIAGRAM IS IN THE DIRECTION OF V_{tr} WITH A MAGNITUDE EQUAL TO V_{tr}/V.

THE VELOCITY MEASUREMENTS WERE MADE IN A PLANE WHICH IS PERPENDICULAR TO THE CENTERLINE OF THE PROPELLER SHAFT AND 7.76 FT AFT OF STA 18½.

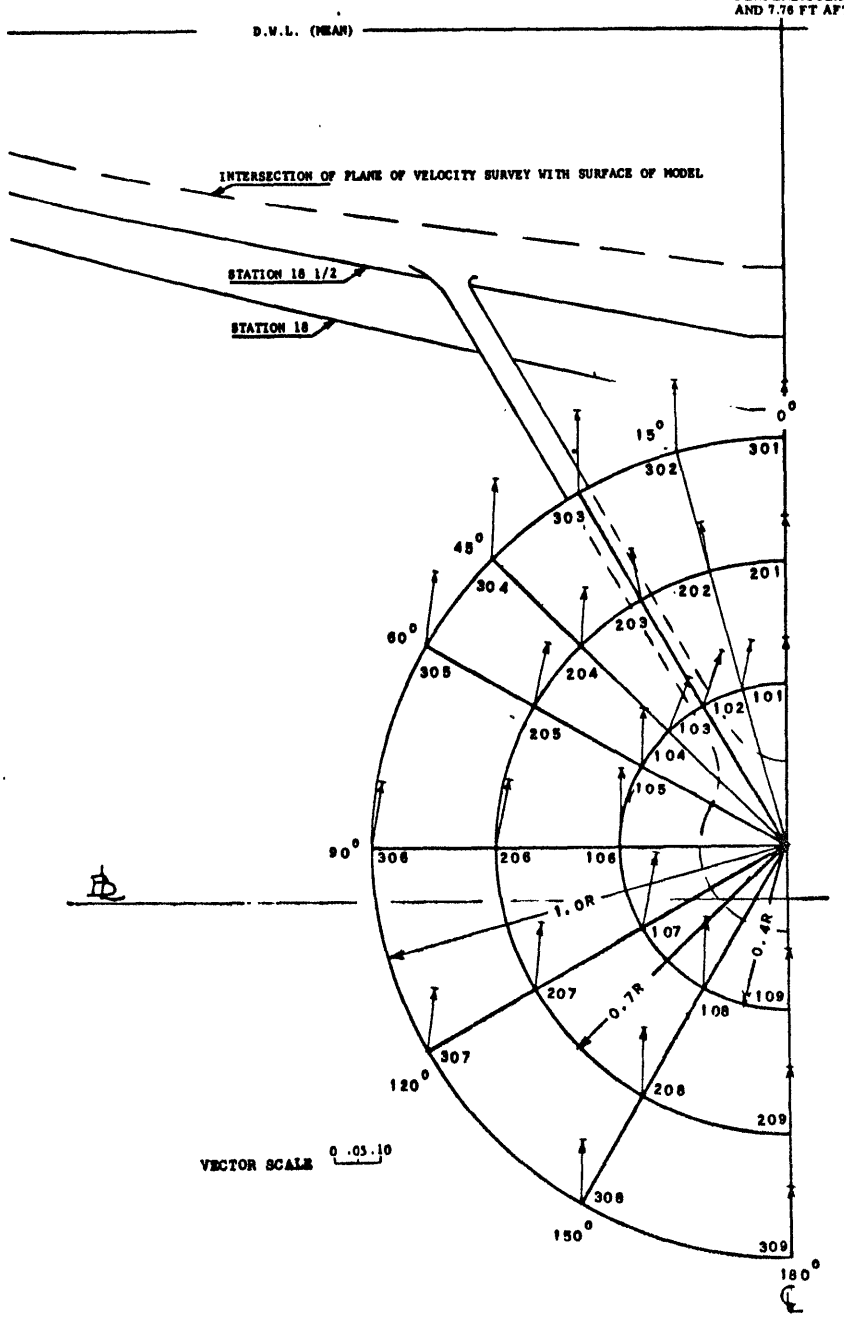

TABLE OF COMPONENT RATIOS

POSITION NUMBER	V_x/V	V_t/V	V_r/V
101	0.993	0	-0.102
102	0.989	-0.048	-0.099
103	0.989	-0.910	-0.079
104	0.998	-0.122	-0.054
105	1.007	-0.146	-0.023
106	1.007	-0.179	0.005
107	1.013	-0.133	0.111
108	1.021	-0.078	0.144
109	1.025	0	0.158
201	0.948	0	-0.098
202	0.963	-0.009	-0.109
203	0.984	-0.047	-0.191
204	0.992	-0.100	-0.066
205	0.995	-0.137	-0.047
206	0.999	-0.154	0.027
207	0.999	-0.122	0.088
208	1.005	-0.068	0.130
209	1.008	0	0.144
301	0.910	0	-0.120
302	0.908	-0.039	-0.153
303	0.910	-0.093	-0.160
304	0.941	-0.133	-0.115
305	0.982	-0.153	-0.064
306	0.995	-0.150	0.022
307	0.994	-0.116	0.083
308	0.998	-0.064	0.123
309	1.001	0	0.136

Figure 7 - Wake Velocity Diagram and Test Data, Model 4773

VELOCITY SURVEY IN WAY OF THE PROPELLER
SINGLE SCREW SHIPS
DE TYPE
MODEL 4870
MODEL DIMENSIONS
LENGTH (LWL) 19 98 FT
BEAM 2.24 FT
DRAFT .743 FT
DISPLACEMENT .452 TONS F.W.
PROPELLER DIAMETER .737 FT
SPEED 6.11 KT
TEST 3
JULY 1961

r, R IS THE DISTANCE FROM THE PROPELLER AXIS (r) EXPRESSED AS A RATIO OF THE PROPELLER AXIS (R)

θ IS THE ANGLE MEASURED FROM THE TOP OF THE PROPELLER DISK IN A COUNTERCLOCKWISE DIRECTION

V IS THE SHIP SPEED

V_x IS THE LONGITUDINAL (NORMAL TO THE PLANE OF SURVEY) COMPONENT OF THE WATER VELOCITY AND IS POSITIVE IN THE ASTERN DIRECTION

V_t IS THE TANGENTIAL COMPONENT OF THE WATER VELOCITY AND IS POSITIVE IN THE COUNTERCLOCKWISE DIRECTION

V_r IS THE RADIAL COMPONENT OF THE WATER VELOCITY AND IS POSITIVE TOWARD THE SHAFT CENTERLINE

V_{tr} IS THE TRANSVERSE COMPONENT OF THE WATER VELOCITY AND IS THE VECTOR SUM OF V_t and V_r.

THE VECTOR SHOWN IN THE DIAGRAM IS IN THE DIRECTION OF V_{tr} WITH A MAGNITUDE EQUAL TO V_{tr}/V

THE VELOCITY MEASUREMENTS WERE MADE IN A PLANE WHICH IS PERPENDICULAR TO THE CENTERLINE OF THE PROPELLER SHAFT AND IS 1 15 FT FWD OF STA 19 AT THE CENTERLINE OF THE SHAFT.

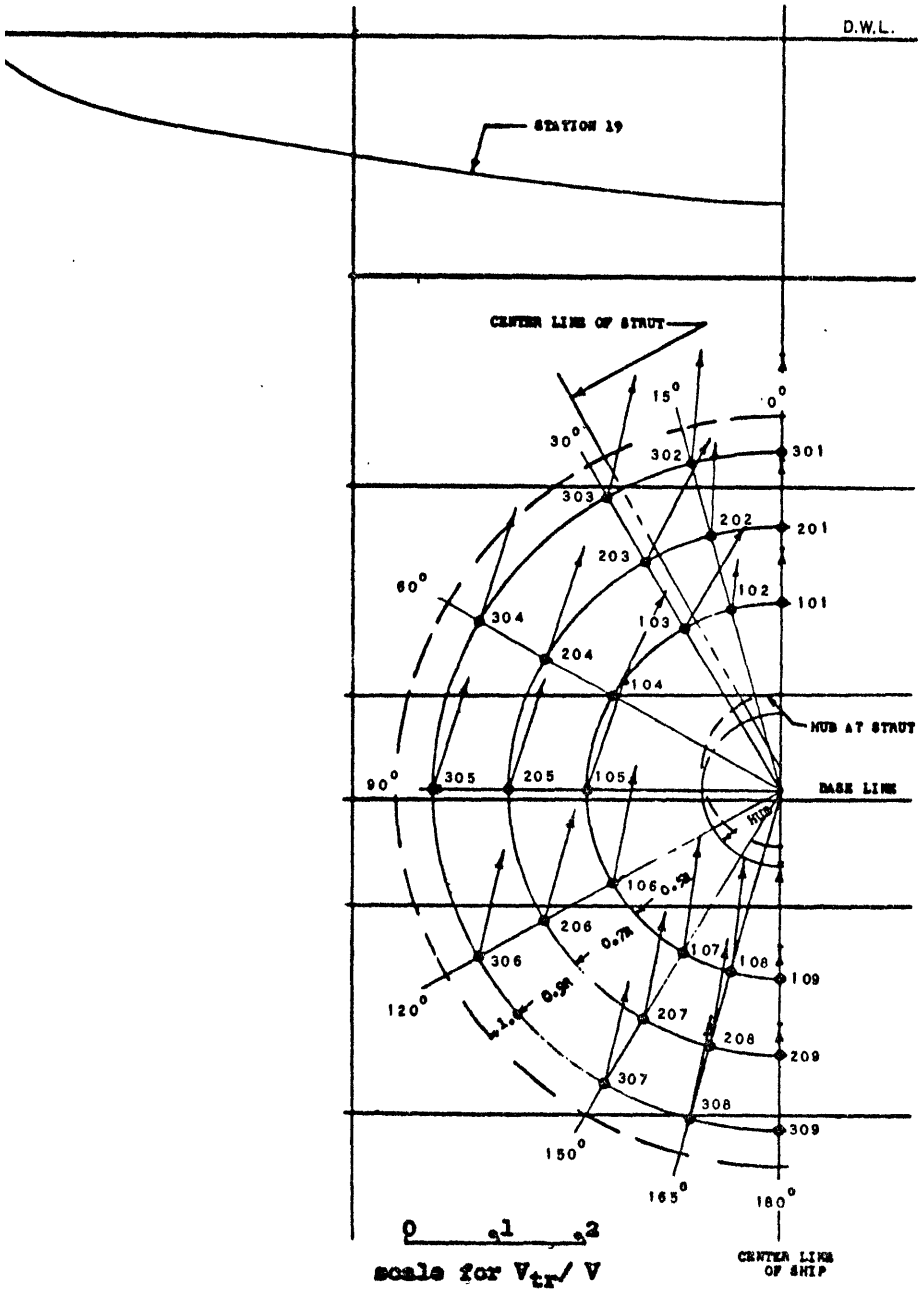

TABLE OF COMPONENT RATIOS

POSITION NUMBER	V_x/V	V_t/V	V_r/V
101	0.934	0	-0.067
102	0.926	0.002	-0 074
103	0.911	-0.189	-0.066
104	1.004	-0.132	-0.030
105	1.005	-0.143	0.032
106	1.009	-0.119	0.083
107	1.006	-0.062	0.114
108	1.011	-0.032	0.123
109	1.010	0	0.126
201	0.924	0	-0.081
202	0.947	-0.039	-0.122
203	1.005	-0.134	-0.105
204	0.994	-0.128	-0.042
205	0.992	-0.132	0.025
206	0.999	-0.108	0.078
207	1.002	-0.061	0 111
208	1.004	-0.027	0.122
209	1.005	0	0.123
301	0.937	0	-0 111
302	0.972	-0.057	-0.126
303	0.973	-0.150	-0.116
304	0.979	-0.131	-0.045
305	0.973	-0.132	0.025
306	0 997	-0.105	0 077
307	0.992	-0.057	0 111
308	0 997	-0.028	0.119
309	0.999	0	0.121

Figure 8 - Wake Velocity Diagram and Test Data, Model 4870

VELOCITY SURVEY IN WAY OF THE PROPELLER
SINGLE SCREW SHIPS
DE TYPE
MODEL 4881
MODEL DIMENSIONS
LENGTH (LWL) 10.06 FT
BEAM 8.24 FT
DRAFT .748 FT
DISPLACEMENT .452 TONS F.W.
PROPELLER DIAMETER .737 FT
SPEED 6.11 KT
TEST 3
JULY 1961

r/R IS THE DISTANCE FROM THE PROPELLER AXIS (r) EXPRESSED AS A RATIO OF THE PROPELLER AXIS (R).

θ IS THE ANGLE MEASURED FROM THE TOP OF THE PROPELLER DISK IN A COUNTERCLOCKWISE DIRECTION.

V IS THE SHIP SPEED

V_x IS THE LONGITUDINAL (NORMAL TO THE PLANE OF SURVEY) COMPONENT OF THE WATER VELOCITY AND IS POSITIVE IN THE ASTERN DIRECTION.

V_t IS THE TANGENTIAL COMPONENT OF THE WATER VELOCITY AND IS POSITIVE IN THE COUNTERCLOCKWISE DIRECTION

V_r IS THE RADIAL COMPONENT OF THE WATER VELOCITY AND IS POSITIVE TOWARD THE SHAFT CENTERLINE.

V_{tr} IS THE TRANSVERSE COMPONENT OF THE WATER VELOCITY AND IS THE VECTOR SUM OF V_t and V_r

THE VECTOR SHOWN IN THE DIAGRAM IS IN THE DIRECTION OF V_{tr} WITH A MAGNITUDE EQUAL TO V_{tr}/V.

THE VELOCITY MEASUREMENTS WERE MADE IN A PLANE WHICH IS PERPENDICULAR TO THE CENTERLINE OF THE PROPELLER SHAFT AND IS 1.15 FT FWD OF STA 19 AT THE CENTERLINE OF THE SHAFT.

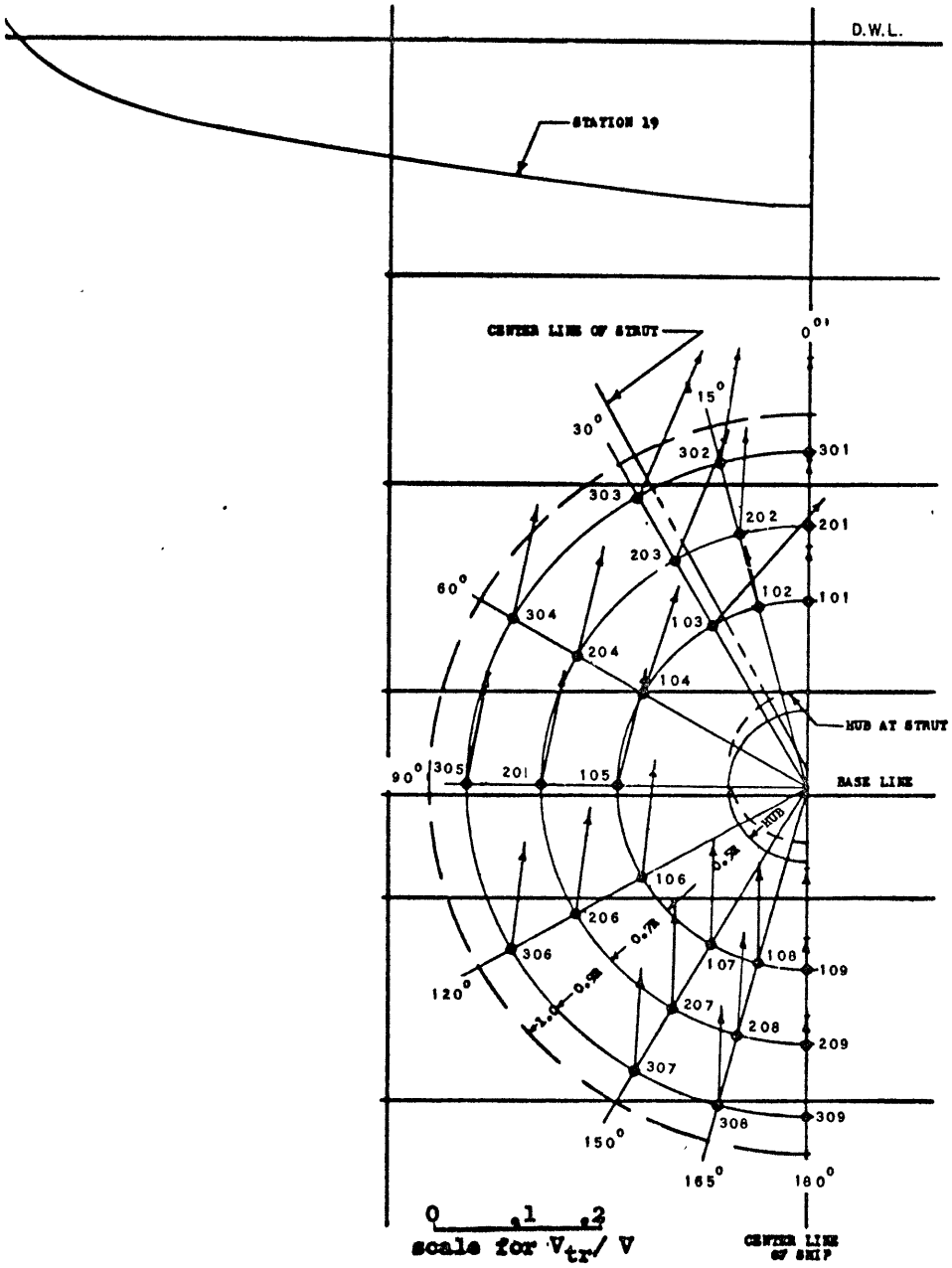

TABLE OF COMPONENT RATIOS

POSITION NUMBER	V_x/V	V_t/V	V_r/V
101	0.905	0	-0.053
102	0.911	-0 022	-0.057
103	0.999	-0.122	-0.072
104	0.994	-0.141	-0.012
105	1.000	-0.141	0.049
106	0.999	-0.107	0.093
107	1.000	-0.052	0.126
108	1.003	-0.018	0.134
109	0.980	0	0.135
201	0.918	0	-0.092
202	0.949	-0.031	-0.106
203	0.994	-0.136	-0.090
204	0.982	-0.136	-0.029
205	0.993	-0.132	0.040
206	0.998	-0.096	0.096
207	0.998	-0.042	0.123
208	0.998	-0.014	0 129
209	0.994	0	0.127
301	0 925	0	-0.114
302	0.970	-0.047	-0.127
303	0 969	-0.098	-0.109
304	0.970	-0 137	-0 031
305	0.979	-0.129	0.042
306	0 989	-0.093	0.087
307	0.994	-0.037	0.119
308	0.970	-0.010	0.124
309	0 988	0	0.123

Figure 9 - Wake Velocity Diagram and Test Data, Model 4881

VELOCITY SURVEY IN WAY OF THE PROPELLER
SINGLE SCREW SHIPS
DE TYPE
MODEL 4954

MODEL DIMENSIONS

LENGTH (LWL)	20 21 FT
BEAM	2.28 FT
DRAFT	726 FT
DISPLACEMENT	.451 TONS F W.
PROPELLER DIAMETER	.768 FT
SPEED	6.11 KT

TEST 7
JULY 1963

r R IS THE DISTANCE FROM THE PROPELLER AXIS (r) EXPRESSED AS A RATIO OF THE PROPELLER AXIS (R)

θ IS THE ANGLE MEASURED FROM THE TOP OF THE PROPELLER DISK IN A COUNTERCLOCKWISE DIRECTION

V IS THE SHIP SPEED.

V_x IS THE LONGITUDINAL (NORMAL TO THE PLANE OF SURVEY) COMPONENT OF THE WATER VELOCITY AND IS POSITIVE IN THE ASTERN DIRECTION

V_t IS THE TANGENTIAL COMPONENT OF THE WATER VELOCITY AND IS POSITIVE IN THE COUNTERCLOCKWISE DIRECTION

V_r IS THE RADIAL COMPONENT OF THE WATER VELOCITY AND IS POSITIVE TOWARD THE SHAFT CENTERLINE.

V_{tr} IS THE TRANSVERSE COMPONENT OF THE WATER VELOCITY AND IS THE VECTOR SUM OF V_t and V_r.

THE VECTOR SHOWN IN THE DIAGRAM IS IN THE DIRECTION OF V_{tr} WITH A MAGNITUDE EQUAL TO V_{tr} V.

THE VELOCITY MEASUREMENTS WERE MADE IN A PLANE WHICH IS PERPENDICULAR TO THE CENTERLINE OF THE PROPELLER SHAFT AND INTERSECTS THE SHAFT CENTERLINE 1.5 FT FWD OF STA 19

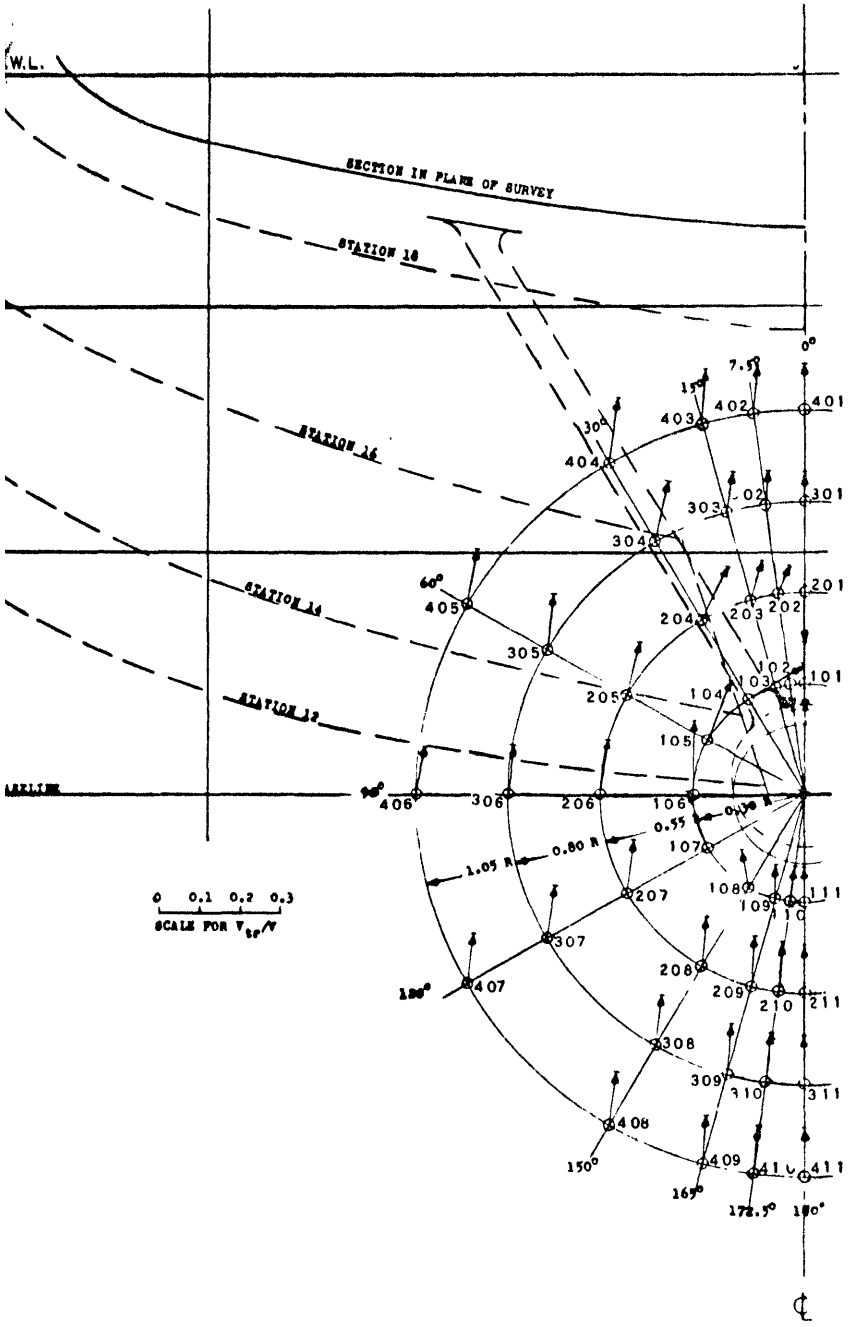

TABLE OF COMPONENT RATIOS

POSITION NUMBER	V_x V	V_t V	V_r V
101	0.876	0	0.064
102	0.974	0	0.064
103	0 857	-0 026	0 057
104	1 031	-0 162	0
105	1.027	-0.160	-0.023
106	1.037	-0.192	-0 002
107	1 048	-0 152	0 030
108	1.045	-0 068	0.078
109	1.034	-0 021	0 088
110	1 035	0	0.095
111	1.034	0	0.096
201	0 905	0	-0 056
202	0 922	-0 036	-0.069
203	0 962	-0.053	-0 085
204	0 999	-0 127	-0 087
205	1 006	-0 133	-0 039
206	1 010	-0 141	0 026
207	1 009	-0.112	0.082
208	1.011	-0 056	0 118
209	1.012	-0.024	0 125
210	1.008	-0.005	0 126
211	1 005	0	0.126
301	0 932	0	-0.074
302	0 930	-0.018	-0.084
303	0.951	-0 047	-0.098
304	0 975	-0 103	-0.117
305	0 987	-0 132	-0.049
306	1 003	-0 135	0 019
307	1 004	-0.104	0.084
308	1 004	-0.051	0 118
309	1 002	-0 021	0 124
310	0 998	-0 003	0.126
311	1 001	0	0.124
401	0 944	0	-0.117
402	0 940	-0 026	-0.118
403	0 953	-0 045	-0 131
404	0 954	-0 103	-0.130
405	0 978	-0 133	-0 045
406	0 998	-0 130	0.021
407	0.998	-0 101	0.077
408	0 993	-0 051	0 112
409	0 994	-0 022	0.120
410	0 990	-0 005	0 121
411	0 993	0	0.122

Figure 10- Wake Velocity Diagram and Test Data, Model 4954

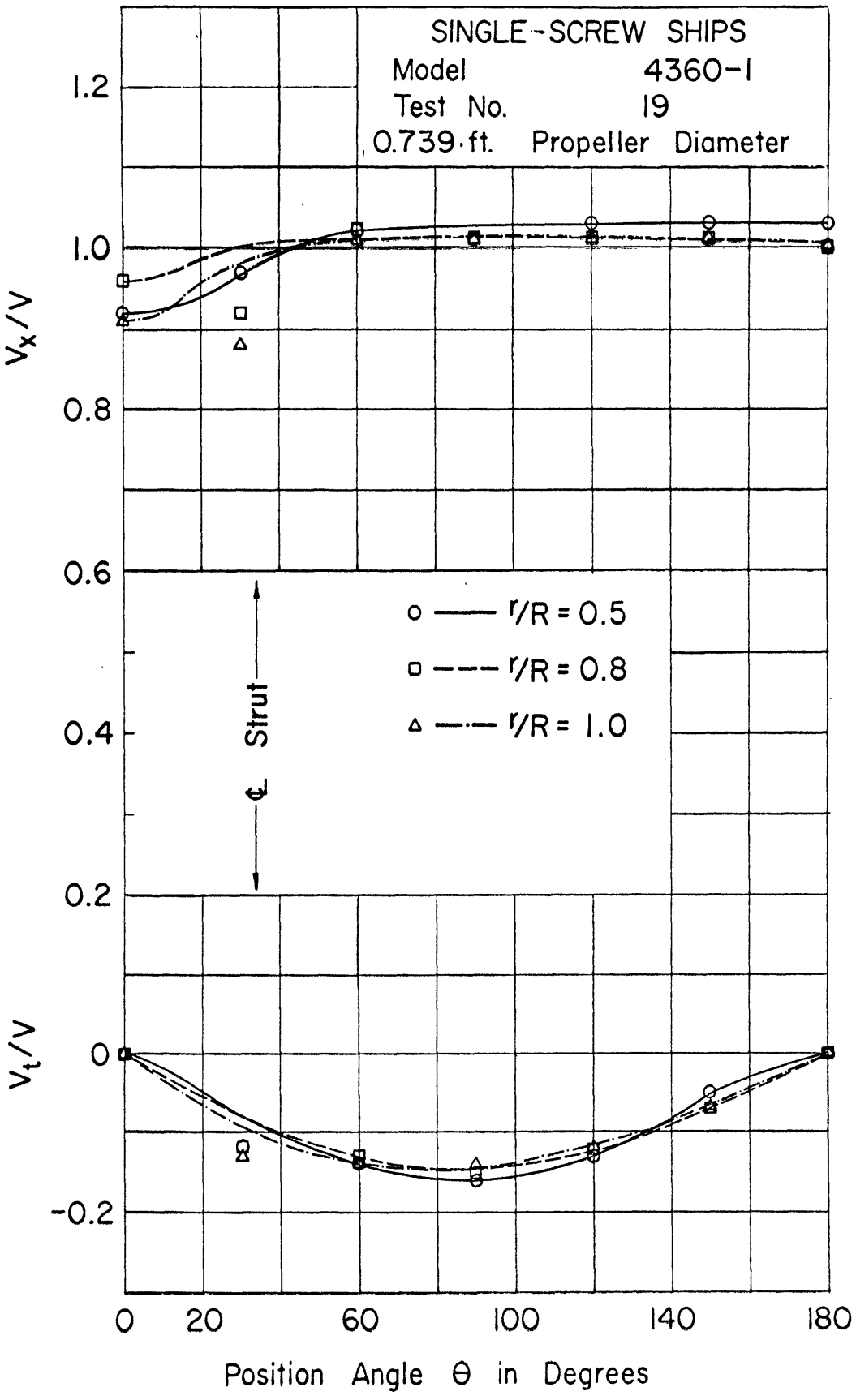

Figure 11- Circumferential Longitudinal (V_x/V) and Tangential (V_t/V) Velocity Distributions at Various Test Radii, Model 4360

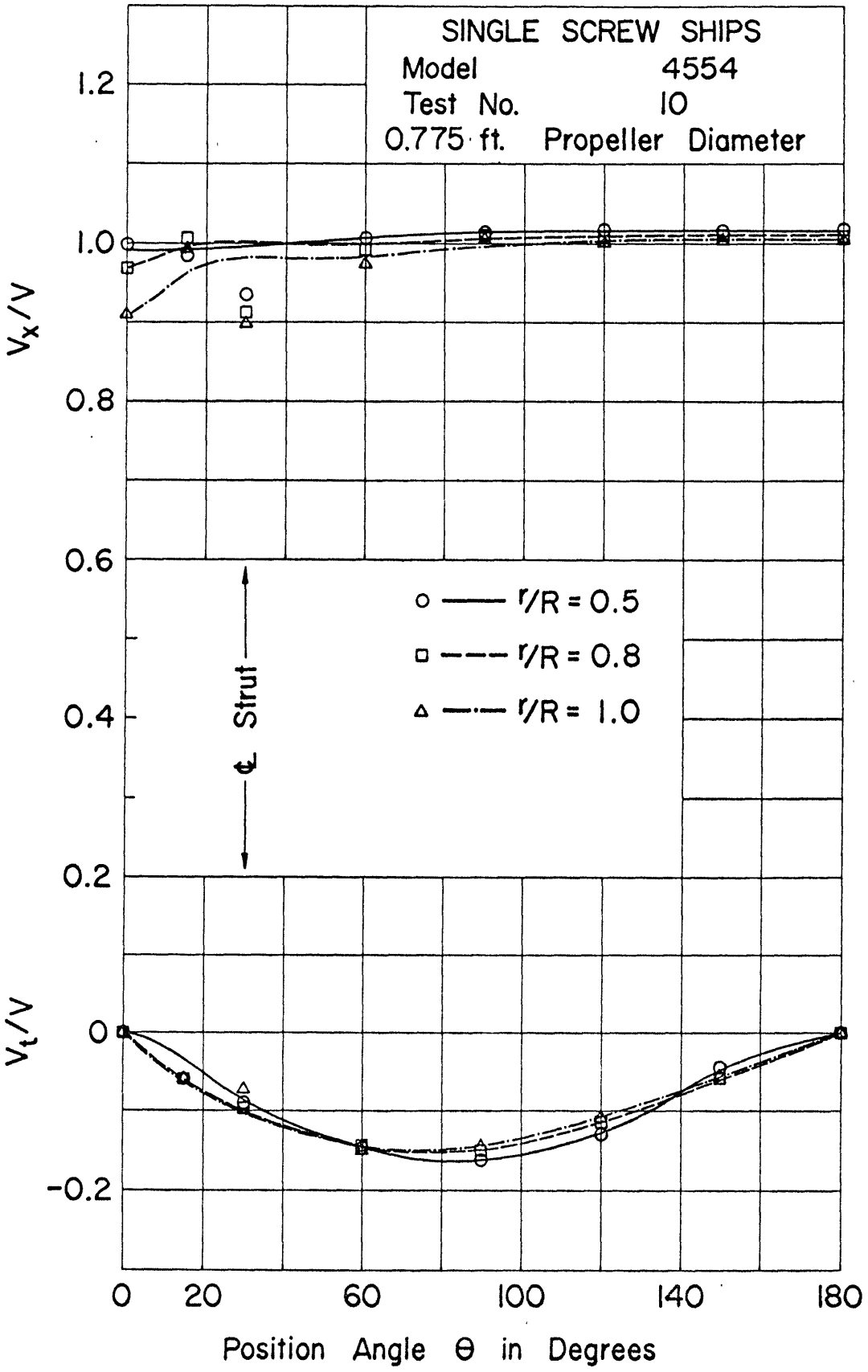

Figure 12- Circumferential Longitudinal (V_x/V) and Tangential (V_t/V) Velocity Distributions at Various Test Radii, Model 4554

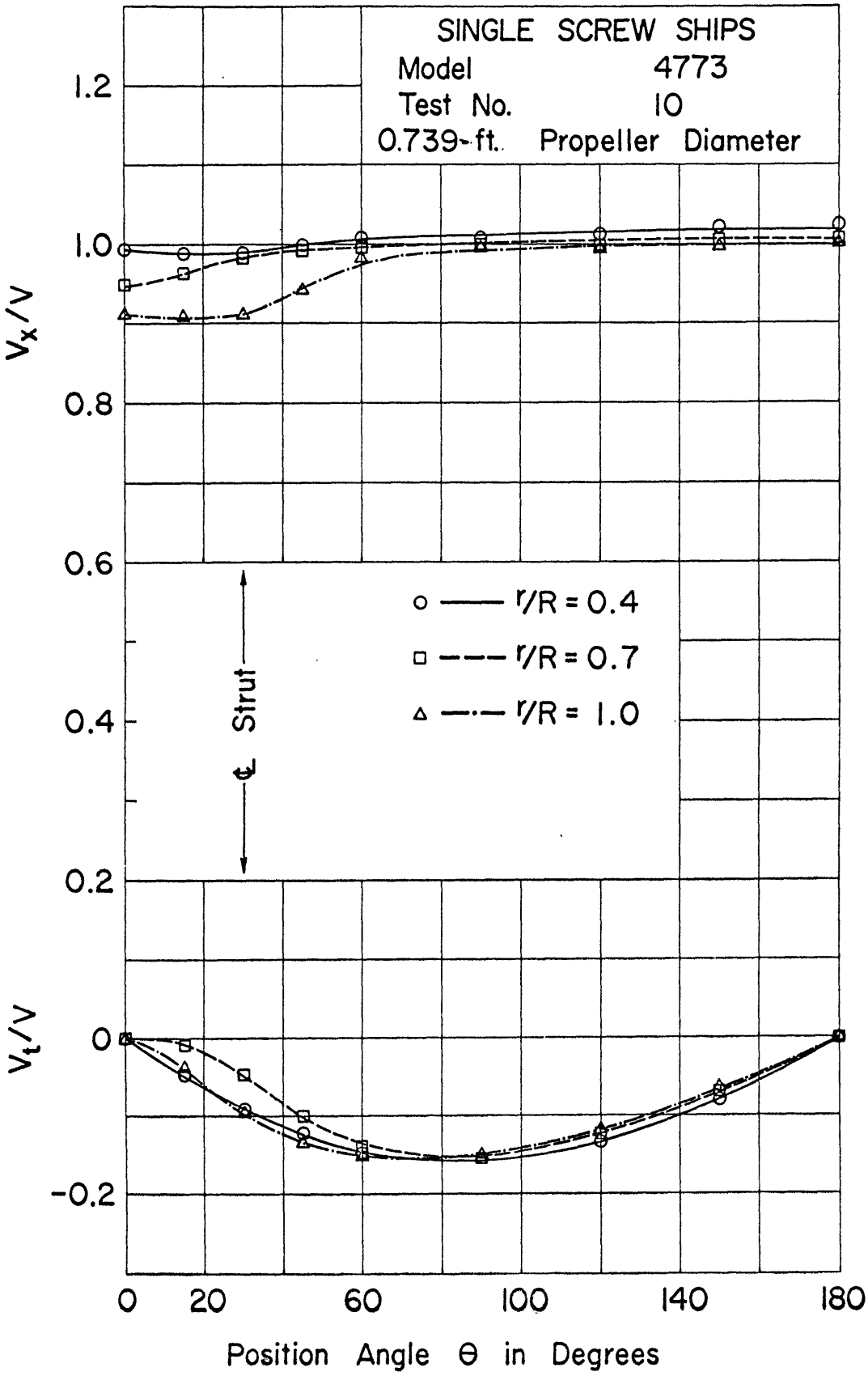

Figure 13- Circumferential Longitudinal (V_x/V) and Tangential (V_t/V) Velocity Distributions at Various Test Radii, Model 4773

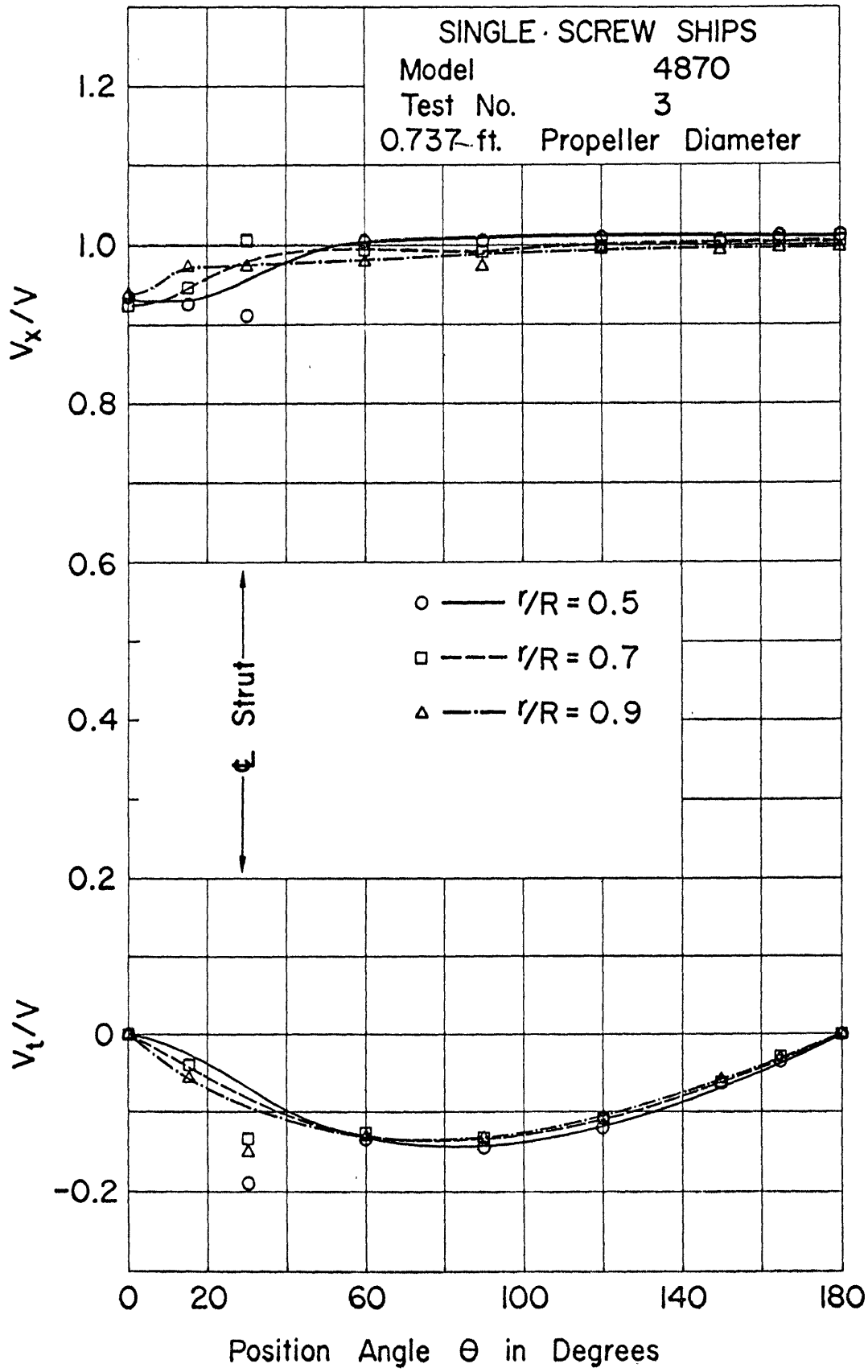

Figure 14- Circumferential Longitudinal (V_x/V) and Tangential (V_t/V) Velocity Distributions at Various Test Radii, Model 4870

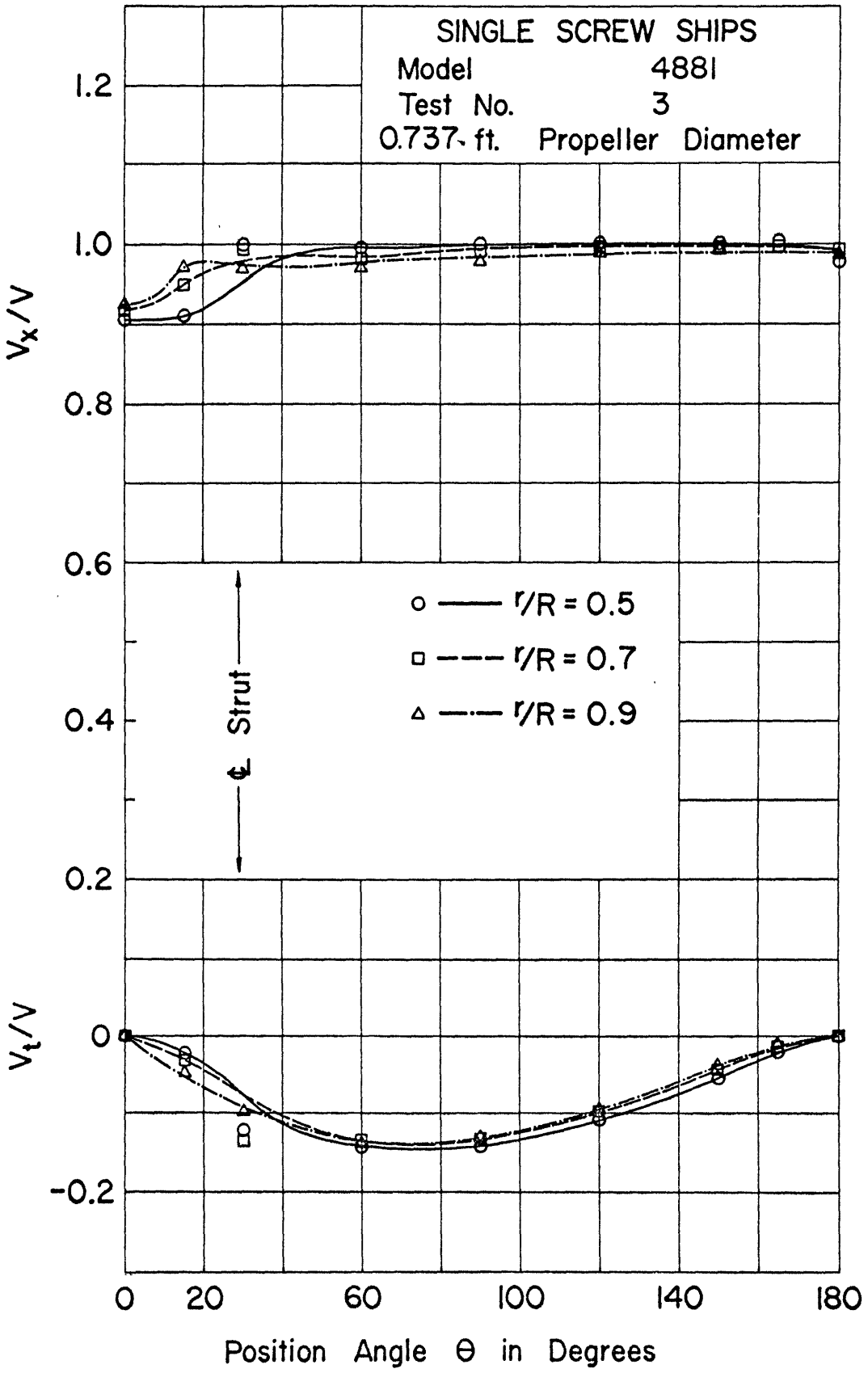

Figure 15- Circumferential Longitudinal (V_x/V) and Tangential (V_t/V) Velocity Distributions at Various Test Radii, Model 4881

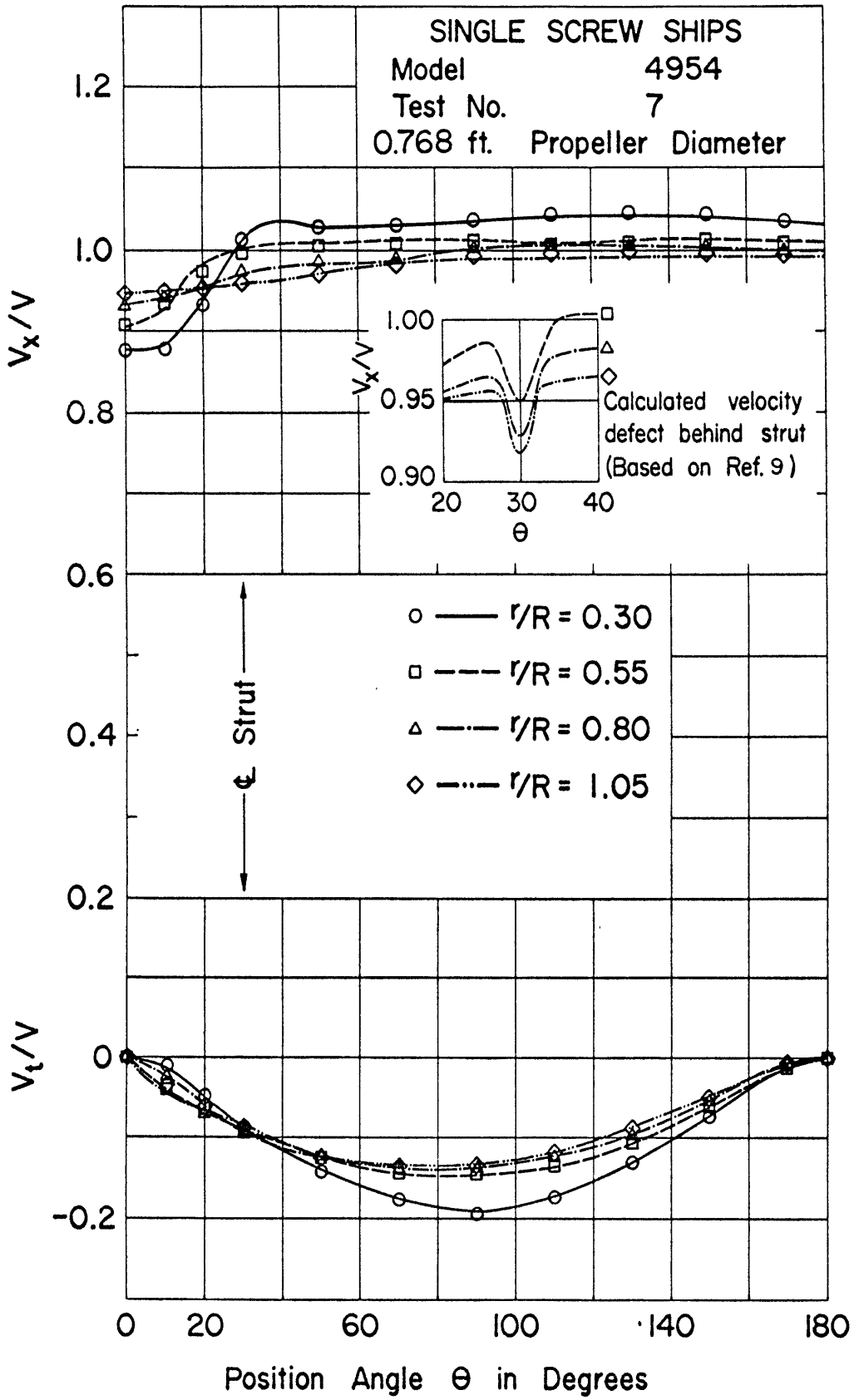

Figure 16- Circumferential Longitudinal (V_x/V) and Tangential (V_t/V) Velocity Distributions at Various Test Radii, Model 4954

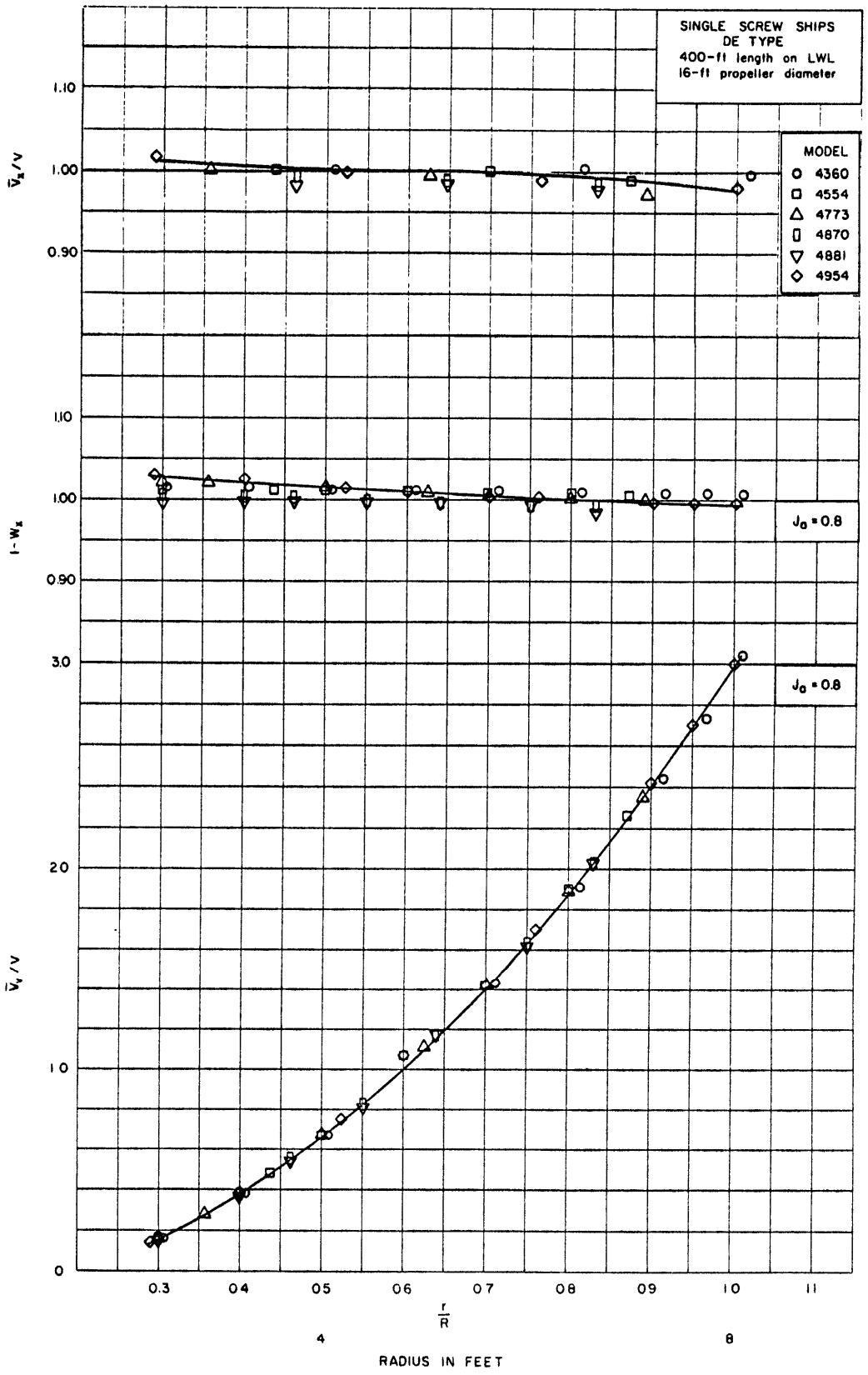

Figure 17- Mean Longitudinal Velocity ($\bar{V}_x/V$), Calculated Volumetric Velocity ($\bar{V}_v/V$) and Volumetric Mean Wake Velocity ($1-W_x$)

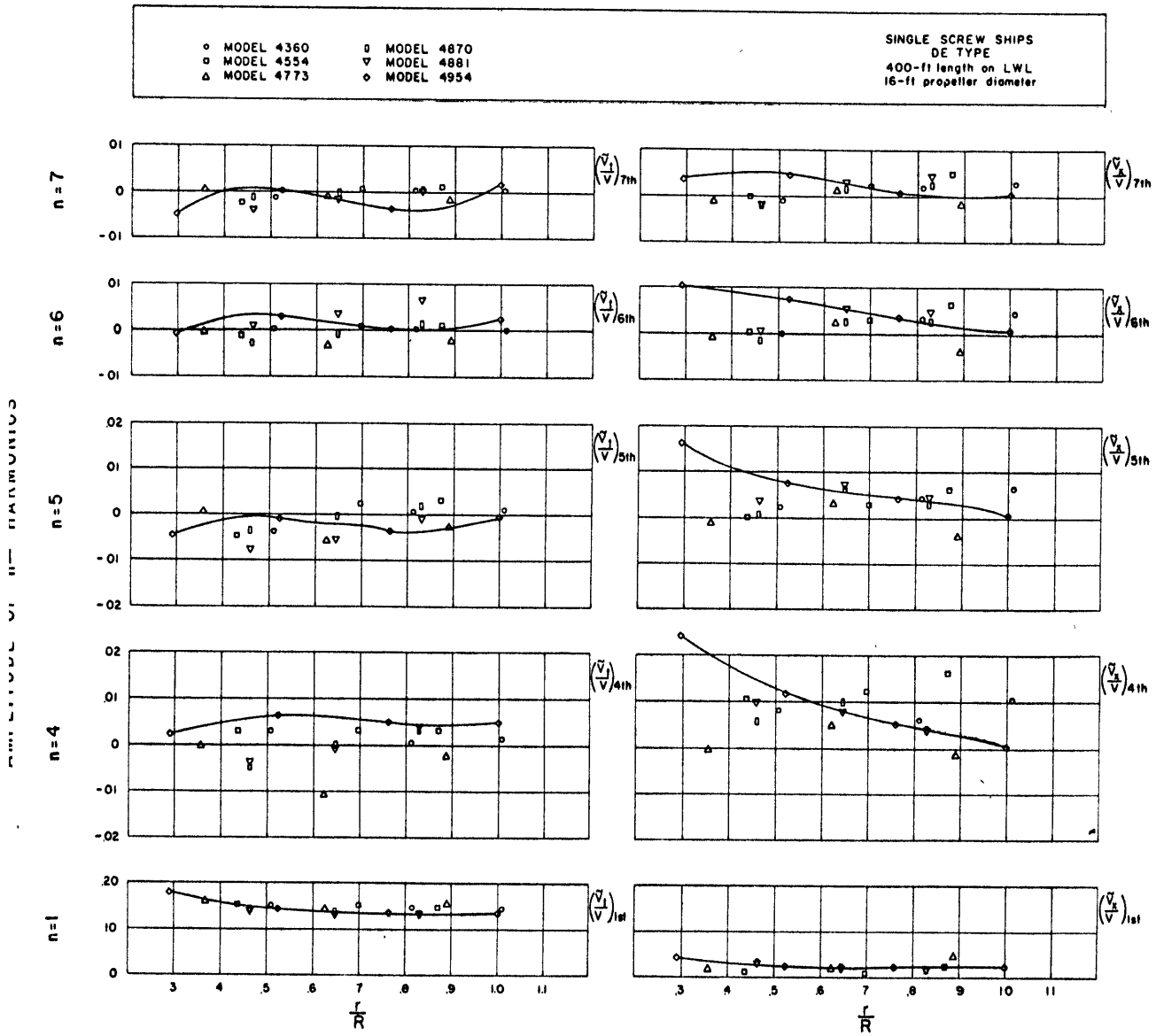

Figure 18- Amplitudes of Various Harmonics of Longitudinal ($\tilde{V}_x/V$) and Tangential ($\tilde{V}_t/V$) Velocity Components

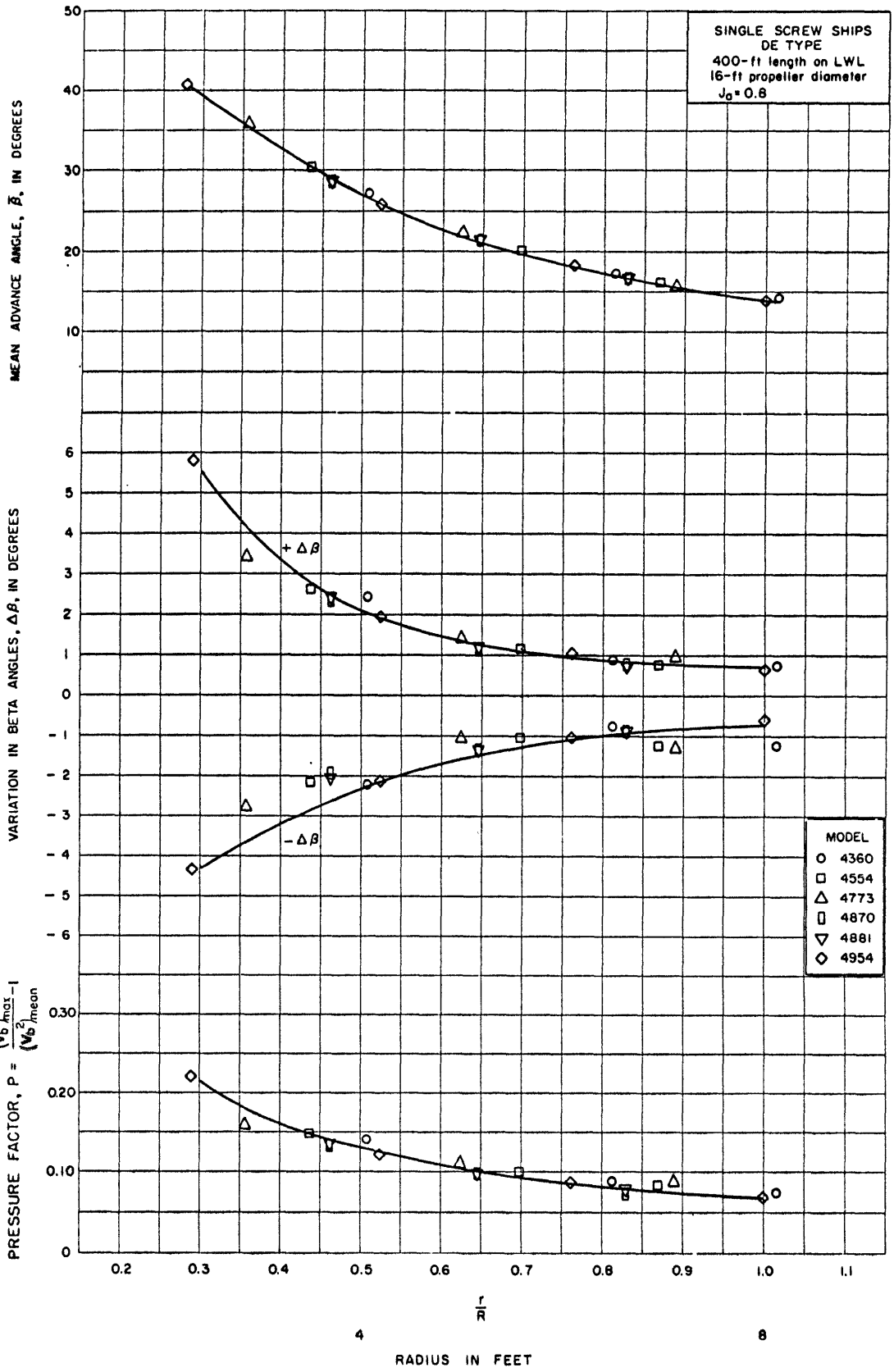

Figure 19- Mean Advance Angle ($\bar{\beta}$), Variations in Beta Angle ($\Delta\beta$) ar Pressure Factor (P)

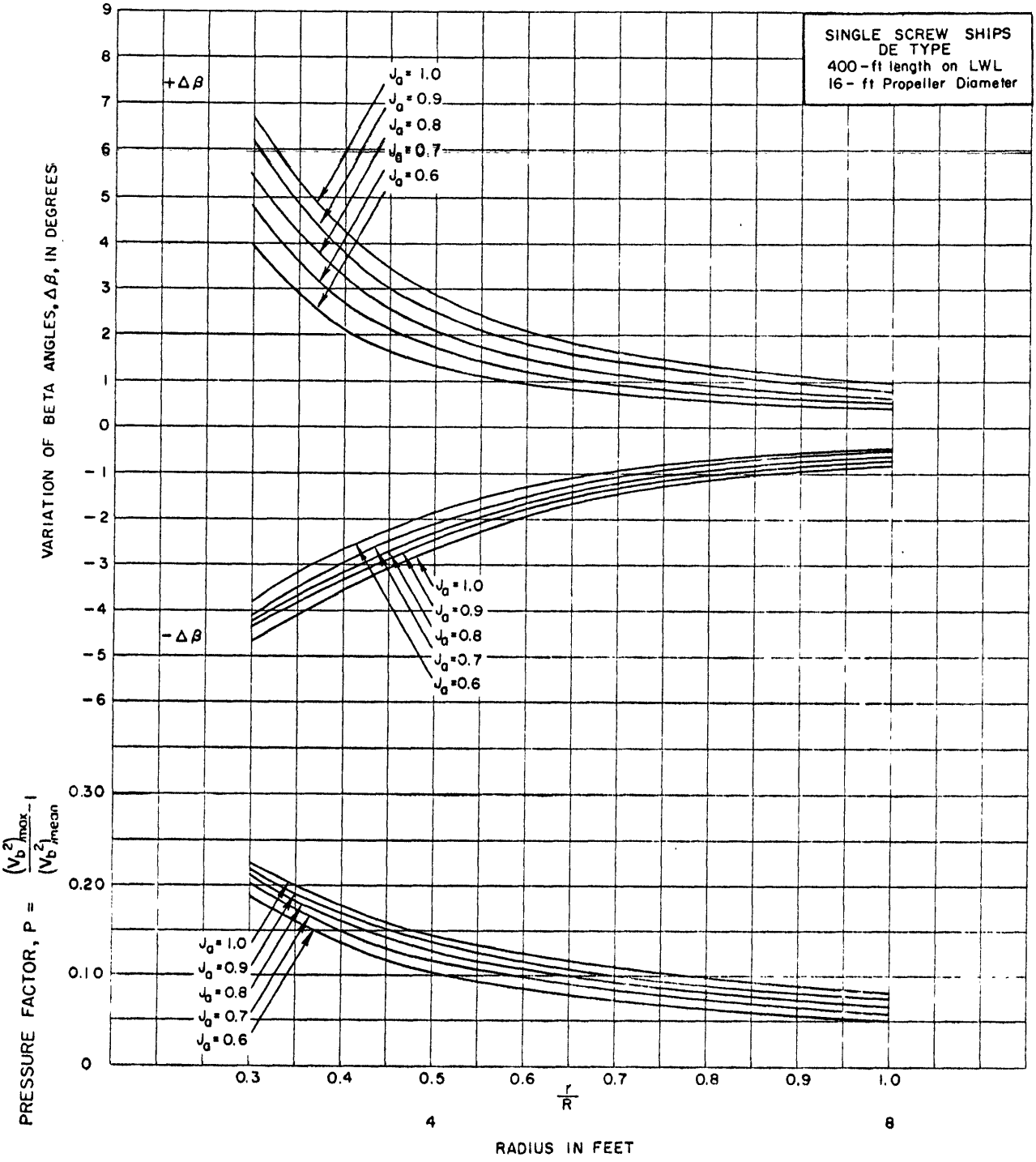

Figure 20- Variation in Beta Angle ($\Delta\beta$) and Pressure Factor (P) for Various J_a Values

INITIAL DISTRIBUTION

Copies		
13	CHBUSHIPS	
	3	Tech Lib (Code 210-L)
	1	Appl Res (Code 340)
	1	Prelim Des (Code 420)
	1	Mach Sci & Res (Code 436)
	1	Hull Des (Code 440)
	1	Prop Shaft & Brng (Code 644)
	1	Lab Mgt (Code 320)
	1	Ship Silencing Br (Code 345)
	1	Cruisers and Destroyers Br (Code 523)
	2	Sci & Res (Code 442)
1	CHBUWEPS	
	1	Library (DLI-3)
3	CHONR	
	2	Fluid Dyn Br (Code 438)
	1	Library (Code 740)
1	SUPT, USNAVPGSCOL	
1	DIR, ORL	
1	ADMIN, Maritime Admin	
20	DDC	
1	SNAME	
1	HD, NAME, MIT	
1	DIR, Iowa Inst. of Hydraulic Res	
1	DIR, St. Anthony Falls Hydraulic Lab	
1	DIR, Davidson Lab, SIT	
1	HD, Dept NAME, Univ of Mich	
1	ADMIN, Inst NAVARCH, Webb	
1	DIR, Inst. of Eng Res, Univ of Calif	

David Taylor Model Basin. Report 1849.
WAKE ANALYSIS OF SHIP MODELS, SINGLE-SCREW DE-TYPE, by H.M. Cheng and J.B. Hadler. Jun 1964. v, 39p. illus., graphs, diagr., tables, refs. UNCLASSIFIED

This report presents the results of an analysis of the wake of single-screw DE-type ship models using the IBM 7090 computer. The data presented are the interpolated longitudinal and tangential velocity distributions, their computed mean values, the harmonic contents of these velocity components, the resultant inflow velocity distribution, and the advance angles and their variations. Also included are the calculated volumetric wake velocities.

1. Ship models--Wake--Mathematical analysis
2. Escort vessels--Wake--Model tests
3. Digital computers--IBM 7090--Application
I. Cheng, Henry M.
II. Hadler, Jacques B.

David Taylor Model Basin. Report 1849.
WAKE ANALYSIS OF SHIP MODELS, SINGLE-SCREW DE-TYPE, by H.M. Cheng and J.B. Hadler. Jun 1964. v, 39p. illus., graphs, diagr., tables, refs. UNCLASSIFIED

This report presents the results of an analysis of the wake of single-screw DE-type ship models using the IBM 7090 computer. The data presented are the interpolated longitudinal and tangential velocity distributions, their computed mean values, the harmonic contents of these velocity components, the resultant inflow velocity distribution, and the advance angles and their variations. Also included are the calculated volumetric wake velocities.

1. Ship models--Wake--Mathematical analysis
2. Escort vessels--Wake--Model tests
3. Digital computers--IBM 7090--Application
I. Cheng, Henry M.
II. Hadler, Jacques B.

David Taylor Model Basin. Report 1849.
WAKE ANALYSIS OF SHIP MODELS, SINGLE-SCREW DE-TYPE, by H.M. Cheng and J.B. Hadler. Jun 1964. v, 39p. illus., graphs, diagr., tables, refs. UNCLASSIFIED

This report presents the results of an analysis of the wake of single-screw DE-type ship models using the IBM 7090 computer. The data presented are the interpolated longitudinal and tangential velocity distributions, their computed mean values, the harmonic contents of these velocity components, the resultant inflow velocity distribution, and the advance angles and their variations. Also included are the calculated volumetric wake velocities.

1. Ship models--Wake--Mathematical analysis
2. Escort vessels--Wake--Model tests
3. Digital computers--IBM 7090--Application
I. Cheng, Henry M.
II. Hadler, Jacques B.

David Taylor Model Basin. Report 1849.
WAKE ANALYSIS OF SHIP MODELS, SINGLE-SCREW DE-TYPE, by H.M. Cheng and J.B. Hadler. Jun 1964. v, 39p. illus., graphs, diagr., tables, refs. UNCLASSIFIED

This report presents the results of an analysis of the wake of single-screw DE-type ship models using the IBM 7090 computer. The data presented are the interpolated longitudinal and tangential velocity distributions, their computed mean values, the harmonic contents of these velocity components, the resultant inflow velocity distribution, and the advance angles and their variations. Also included are the calculated volumetric wake velocities.

1. Ship models--Wake--Mathematical analysis
2. Escort vessels--Wake--Model tests
3. Digital computers--IBM 7090--Application
I. Cheng, Henry M.
II. Hadler, Jacques B.

David Taylor Model Basin. Report 1849.
WAKE ANALYSIS OF SHIP MODELS, SINGLE-SCREW DE-TYPE, by H.M. Cheng and J.B. Hadler. Jun 1964. v, 39p. illus., graphs, diagr., tables, refs. UNCLASSIFIED

This report presents the results of an analysis of the wake of single-screw DE-type ship models using the IBM 7090 computer. The data presented are the interpolated longitudinal and tangential velocity distributions, their computed mean values, the harmonic contents of these velocity components, the resultant inflow velocity distribution, and the advance angles and their variations. Also included are the calculated volumetric wake velocities.

1. Ship models--Wake--Mathematical analysis
2. Escort vessels--Wake--Model tests
3. Digital computers--IBM 7090--Application
I. Cheng, Henry M.
II. Hadler, Jacques B.

David Taylor Model Basin. Report 1849.
WAKE ANALYSIS OF SHIP MODELS, SINGLE-SCREW DE-TYPE, by H.M. Cheng and J.B. Hadler. Jun 1964. v, 39p. illus., graphs, diagr., tables, refs. UNCLASSIFIED

This report presents the results of an analysis of the wake of single-screw DE-type ship models using the IBM 7090 computer. The data presented are the interpolated longitudinal and tangential velocity distributions, their computed mean values, the harmonic contents of these velocity components, the resultant inflow velocity distribution, and the advance angles and their variations. Also included are the calculated volumetric wake velocities.

1. Ship models--Wake--Mathematical analysis
2. Escort vessels--Wake--Model tests
3. Digital computers--IBM 7090--Application
I. Cheng, Henry M.
II. Hadler, Jacques B.

David Taylor Model Basin. Report 1849.
WAKE ANALYSIS OF SHIP MODELS, SINGLE-SCREW DE-TYPE, by H.M. Cheng and J.B. Hadler. Jun 1964. v, 39p. illus., graphs, diagr., tables, refs. UNCLASSIFIED

This report presents the results of an analysis of the wake of single-screw DE-type ship models using the IBM 7090 computer. The data presented are the interpolated longitudinal and tangential velocity distributions, their computed mean values, the harmonic contents of these velocity components, the resultant inflow velocity distribution, and the advance angles and their variations. Also included are the calculated volumetric wake velocities.

1. Ship models--Wake--Mathematical analysis
2. Escort vessels--Wake--Model tests
3. Digital computers--IBM 7090--Application
I. Cheng, Henry M.
II. Hadler, Jacques B.

David Taylor Model Basin. Report 1849.
WAKE ANALYSIS OF SHIP MODELS, SINGLE-SCREW DE-TYPE, by H.M. Cheng and J.B. Hadler. Jun 1964. v, 39p. illus., graphs, diagr., tables, refs. UNCLASSIFIED

This report presents the results of an analysis of the wake of single-screw DE-type ship models using the IBM 7090 computer. The data presented are the interpolated longitudinal and tangential velocity distributions, their computed mean values, the harmonic contents of these velocity components, the resultant inflow velocity distribution, and the advance angles and their variations. Also included are the calculated volumetric wake velocities.

1. Ship models--Wake--Mathematical analysis
2. Escort vessels--Wake--Model tests
3. Digital computers--IBM 7090--Application
I. Cheng, Henry M.
II. Hadler, Jacques B.

MIT LIBRARIES DUPL
3 9080 02753 0291